BUCKLING OF INHOMOGENEOUS AND FUNCTIONALLY GRADED COLUMNS

by

Mohammed Ghassan Aldadah

A Thesis Presented to the Faculty of the
American University of Sharjah
College of Engineering
in Partial Fulfillment
of the Requirements
for the Degree of

Master of Science in
Mechanical Engineering

Sharjah, United Arab Emirates

July 2014

Approval Signatures

We, the undersigned, approve the Master's Thesis of Mohammed Ghassan Aldadah

Thesis Title: Buckling of Inhomogeneous and Functionally Graded Columns

Signature	**Date of Signature** (dd/mm/yyyy)

_____   _____
Dr. Shivakumar Ranganathan
Assistant Professor, Department of Mechanical Engineering
Thesis Advisor

_____   _____
Dr. Farid Abed
Associate Professor, Department of Civil Engineering
Thesis Co-Advisor

_____   _____
Dr. Bassam Abu-Nabah
Assistant Professor, Department of Mechanical Engineering
Thesis Committee Member

_____   _____
Dr. Noha Hussein
Associate Professor, Department of Industrial Engineering
Thesis Committee Member

_____   _____
Dr. Essam Wahba
Interim Head, Department of Mechanical Engineering

_____   _____
Dr. Hany El-Kadi
Associate Dean, College of Engineering

_____   _____
Dr. Leland Blank
Dean, College of Engineering

_____   _____
Dr. Khaled Assaleh
Director of Graduate Studies

Acknowledgements

In the name of Allah, the most gracious and most merciful.

First, I am most grateful to Allah for granting me the power and will to carry on and complete this research. In addition, I would like to express my appreciation and gratitude to Dr. Shivakumar Ranganathan, my thesis advisor, and Dr. Farid Abed, my thesis co-advisor, for their support when needed and their continued teachings and constant encouragement to help me improve.

I am also thankful to my family for supporting and helping me while I finished my master's degree.

Additional thanks to Ahmed Dalaq and Bharath for helping me in learning how to link between MATLAB and ABAQUS software and special thanks to Emad Kishta for teaching me ABAQUS basics. My thanks also go the American University of Sharjah and especially to the Department of Mechanical Engineering for supplying the labs and equipment used in this research. Furthermore, I would like to thank Ms. Salwa Mohamed for her guidance throughout this research and during my graduate studies. Finally, I would like to express my sincere thanks and gratitude to my friends for the unconditional support.

To my beloved family

Abstract

Buckling is an instability encountered in a wide variety of problems, both in engineering and biology. Almost all engineering structures are designed with adequate safety factors to prevent failure due to buckling, yielding, or dynamic loads. In a classical sense, design for buckling is done by carefully controlling the modulus of elasticity, moment of inertia, and the length of the structure. Further, such an approach assumes the material to be homogeneous and does not generally account for the microstructural details of the column. In the first part of this thesis, we study the buckling of inhomogeneous columns with a two-phase checkerboard microstructure. Monte Carlo simulations are used to generate microstructures with arbitrary volume fractions and phase contrasts (ratio of the modulus of individual phases). An analytical form is obtained for the ensemble averaged critical buckling load based on the results of over 18,000 eigenvalue problems at arbitrary volume fractions, phase contrasts, and distributions. Further, microstructural realizations that correspond to the highest buckling load (best design) and the lowest buckling load (worst design) are identified and the corresponding distribution of individual phases is determined. The statistical nature of the critical buckling load is discussed by computing the statistical moments that include the mean, coefficient of variation, skewness, and kurtosis. Next, we consider the buckling of long and slender columns with functionally graded microstructure. In such columns, the modulus of elasticity and/or the moment of inertia is varied in a controlled manner along the length of the column. The primary objective is to identify functionally graded microstructures that maximize (and minimize) the critical buckling load when compared to a reference homogeneous column. Several columns with a variety of microstructures are examined and a constraint is imposed on each of the microstructures so that the volume averaged elastic modulus remains the same in all the columns. The buckling load capacity of these microstructures is determined using linear perturbation analysis, as well as the Rayleigh-Ritz method. Finally, microstructures that maximize the critical buckling load are identified and a relationship between the material distribution and the corresponding buckling mode shape is established.

Search Terms: Checkerboard, FGM, Buckling capacity, Inhomogeneous

Table of contents

List of figures

List of tables

Nomenclature

$E(x)$	Young modulus of elasticity as a function of length
I	Moment of inertia
v	Deflection
P	Buckling load
C	Boundary condition constant
L	Column length
B	Set of deterministic checkerboard
Ω	Realization space
ω	Specific microstructural realization
χ	Indicator function
$\vec{x}$	Position vector
K	Tangent stiffness matrix
v	Displacement matrix
k	Contrast
$\langle \bullet \rangle$	Ensemble average
α	Volume fraction
Π	Potential energy
K	Flexural rigidity
a,b,c,d	Function parameters
R	Buckling capacity

Subscripts

cr	Critical
c	Rescaled
n	Normalized
hom	Homogenous
In hom	Inhomogeneous

Abbreviations

FPM	Functional Perturbation Method
FGM	Functionally Graded Materials
RR	Rayleigh Ritz method

Chapter 1. Introduction

1.1   Context and motivation

Load bearing structural members are integral part of any engineering design. Designing such members requires satisfaction of certain criteria of strength, deflection, and stability. Adequate safety factors must be provided to prevent failure due to buckling, yielding, or dynamic loads. Slender structural members such as columns typically buckle prior to yielding. Buckling specifically is an instability phenomenon that leads to failure of slender members typically subjected to compressive loads. The most widely used criteria for buckling instability is the Euler's buckling solution, which predicts the maximum axial compressive load that a slender, homogeneous, and ideal column can carry. This solution states the critical buckling load is directly proportional to the modulus of elasticity, area moment of inertia, and boundary conditions, and is inversely proportional to the square of the column length. However, the result is limited to long columns and does not account for material inhomogeneity, in spite the fact that inhomogeneous materials exist everywhere in nature, and that most materials exhibit inhomogeneity when the microstructural details are taken into account. Such materials can also be engineered to design columns with performance better than their homogeneous counterparts (for instance using 3D printing to create a functionally graded microstructure). Thus, there is a clear need to understand the effect of a material's inhomogeneity on the overall response of such columns.

Inhomogeneous materials are composites consisting of two or more materials with variable properties or orientation. Such materials behave differently when compared to their homogeneous counterparts. The focus of this thesis will be specifically on two types of inhomogeneous materials: a) columns with checkerboard microstructure (piecewise continuous), and b) columns with a functionally graded microstructure. In the checkerboard problem, the microstructure of the column is made up of two materials with very different elastic moduli. In the case of a Functionally Graded Materials (FGM), the material property, composition, and orientation is varied gradually over the volume. This guided variation helps in controlling the characteristics of the materials in target applications to enhance the performance and optimize the design of structures. Functionally graded materials can

be used to enhance the buckling capacity by utilizing the distribution of the material in a matter and configuration that resists or counteracts the buckling mode and thus increases the buckling load.

Inhomogeneous materials are currently applied in different fields such as aircraft industries and biomedical industries. In the aircraft industry, space shuttles utilize ceramic tiles for thermal protection from heat generation upon the entry of earth atmosphere [1]. The normal ceramic tiles are prone to cracking due to differences in thermal expansion coefficients. However, if metal-ceramic FGM tiles are used instead, then it will provide better thermal protection and load carrying capabilities thereby decreasing the chances of the tiles cracking. Additionally, because of their thermal properties, FGM materials can be used for aircraft exhaust washes as well. Moreover, in biomedical industries, FGM is being tested as artificial bone implants [2]. An artificial biomaterial for a knee joint replacement is being developed by tailoring an FGM that consists of ultra-high molecular weight polyethylene (UHMWPE) fiber reinforced high-density polyethylene combined with a surface of UHMWPE. In addition, new dental implants are being designed by using FGM this is because it can carry a greater load at a smaller size than the original amalgam being used.

1.2   Objective and scope of work

The aim of this research is to investigate the use of inhomogeneous materials such as checkerboard and functionally graded materials in column design. Additionally, the research aims to identify a closed-form solution for the buckling of checkerboard columns. Finally, optimized distributions of functionally graded materials in columns will be studied. The research will be split into two main subjects areas as follows:

- Buckling of checkerboard type column with the young's modulus defined using indicator functions: $E(\vec{r}) = \chi_1(\vec{r})E_1 + \chi_2(\vec{r})E_2$. Here, $\vec{r}$ is the position vector, E_1 and E_2 are the young's moduli of the individual phases, and $\chi_i(\vec{r})$ is the indicator functions of the region occupied by phase i. This problem will be considered in one, two, and three dimensions, as well as in certain exact analytical solutions.

- An evaluation of the improvement of buckling capacity of FGM columns compared to its homogenous counterpart. In this situation, $E(\vec{r})$ can be interpreted as a Taylor's series expansion about a reference Young's Modulus, E_0.

1.3 Thesis organization

This thesis is organized into five chapters as follows:

Chapter 1 is an introduction to the thesis and includes brief description of the buckling problem and inhomogeneous materials as well as the objectives and scope of work.

Chapter 2 is a literature review on prior research related to the buckling of checkerboard columns and the functionally graded materials.

Chapter 3 is titled "Checkerboard Columns" in which the buckling of inhomogeneous columns with a two-phase checkerboard microstructure is examined. The chapter will also include the results of different checkerboards columns, the corresponding best and worst designs, and the statistical analysis of the data obtained.

Chapter 4 pertains to the buckling of functionally graded columns. It also will show the research methodology used in analyzing and obtaining results. The chapter will include results showing the best functions to be used, the effect of varying homogenous young modulus, and the relationship between the mode shapes and the functionally graded materials.

Chapter 5 will conclude the thesis, summarize the results, and present possible topics for future research.

Chapter 2. Background

2.1   Checkerboard columns

This research is perhaps the first study on the behavior of columns with checkerboard microstructure, although such microstructures have been studied in other areas that pertain to heat conduction, flow through porous media, and planar elasticity. A column with a checkerboard microstructure is made up of two materials with different elastic moduli at arbitrary volume fractions, phase contrasts, and morphology. The most relevant literature to the present study would be the buckling of inhomogeneous columns as discussed in the subsequent paragraphs.

A study by Elishakoff and Rollot investigated columns with variable stiffness [3]. In their study, Euler's buckling equation was modified to allow for variable stiffness across the length of the material. Then using a preselected variable stiffness, the modified Euler equation was solved using Mathematica software to produce possible solution sets in order to obtain the critical buckling load. As a continuation to their study, Elishakoff posed the same problem as an inverse buckling problem [4]. The inverse method, determined the stiffness distribution and the critical buckling load for a non-uniform beam with specified boundary conditions by using a preselected function for the buckling mode. Such a method produces results for certain classes of inhomogeneous materials, and yet it does not provide exact solutions for general heterogeneity. Li derived a solution for the buckling load of non-uniform columns subjected to concentrated axial and distributed loads [5]. In his approach, the governing equations were initially reduced using functional transformation and later solved using Bessel function. The analytical solution provided results for twelve different cases that are important in engineering applications such as high-rise buildings subjected to distributed loads. In yet another study, Huang and Li presented an analytical approach to determine the critical buckling load of a non-uniform column with or without continuous elastic restraint [6]. Their study identified an optimal ratio between the radius in the middle of the cylinder and the radius at the end for maximum carrying load capacity.

Atlus et al. introduced a new method for obtaining the buckling load analytically for linear inhomogeneous materials using the Functional Perturbation Method (FPM) [7]. According to these researchers, the FPM method provided more accurate results

for linear inhomogeneous materials than the conventional Galerkin and Rayleigh-Ritz methods. Along similar lines, Huang and Luo derived a solution for the buckling of inhomogeneous beams by using the power series to represent the mode shapes [8]. The power series method used was illustrated by studying a composite beam under various end supports. In addition, Morimoto et al. investigated the buckling of inhomogeneous rectangular plates subjected to uniform in-plane shear [9]. In their study, an inhomogeneity parameter was introduced which in turn contributed to the bending rigidity. Also, as the inhomogeneity parameter was increased, the buckling load increased but the buckling mode shape remained unaffected.

Furthermore, Earls emphasized on the numerical limitations of using finite element modeling and eigenvalues in the solution of buckling equation [10]. The limitations included differing results for the same structures using different software's and the stability of the results. This indicates the necessity of carefully assisting the finite element solution with closed-form analytical solutions or experiments wherever possible. More recently, Li et al. solved the buckling equation for composite non-uniform columns with distributed axial loads or tip forces. Thereby utilizing the solution to tailor materials such that the ratio of the buckling load to the weight is maximized for axially graded inhomogeneous composite columns with uniform cross-section [11]. The optimization technique was performed on a column with clamped and free ends resulting in the need to increase material density around the free end in order to increase the maximum load carrying capacity. In the problem, Li et al. approximated a non-homogenous column with a piecewise function with constant geometrical and material properties. The resulting eigenvalue problem was then solved using a new numerical algorithm with different boundary conditions.

2.2   Functionally graded materials

Functionally graded materials are composites with variable stiffness or geometry along their length. Elishakoff and Calio investigated the axially graded beam to obtain a generalized solution for columns and beams with functionally graded materials [12]. For simply supported beams, a closed form solution was obtained which indicated that using a semi inverse problem and Rayleigh quotient method can be a very helpful tool in the design of buckling problems. The design method utilized to investigate the axially graded material is dependent on using a pre-selected natural frequency or a

buckling load as a preliminary solution for the problem. Furthermore, Elishakoff compared the solution of Rayleigh Ritz (RR) non-integer power method and the normal Rayleigh-Ritz two-term solution for different cases, such as prismatic cantilever column, stepped column, prismatic column under its own weight, and on a smoothly tapered column [13]. The RR non-integer power method and the normal RR two-term solution is then applied in all the cases mentioned in order to compare both methods and define their usage. The results obtained showed that both methods are accurate with a main difference in the complexity of the solution for the RR non-integer solutions. The solution used in this situation can be used as a bench mark for smoothly tapered columns.

Additionally, Pradhan and Chakraverty performed a free vibration analysis of functionally graded materials subject to a different set of boundary conditions by using RR method [14]. The analysis resulted in the ability to use the RR method in solving FGM, especially when using high number of polynomials. Also, when they deducted this the FGM beams behaved in a similar manner to the isotropic beam despite the changes in boundary conditions and the complications of material properties and configuration. Likewise, Sankar obtained an elastic solution for FGM sinusoidal transverse loading. The FGM beam was designed to vary in an exponential manner [15]. One of the key findings stated the stress concentration, in case of the FGM, is dependent on the soft or hard face of the FG thereby indicating the need to distribute the material in a manner that equalizes the stress concentration. Along similar lines, Elishakoff and Miglis studied a clamped-free beam with compressive loadings on the free edge [16].The study involved solving a semi inverse problem of buckling of a functionally graded beam with only the young modulus varying along the beam. The study resulted in an interesting behavior of the beam where three different buckling modes occurred for the same load. These results could either indicate a special phenomenon for the buckling of inhomogeneous materials or the existence of a great deal of numerical instabilities. Yet the results were very intriguing as it it ended up showing inhomogeneous materials had different properties than normal homogenous materials; this was of interest for further studies. Huang and Li developed a new approach to solve free vibrations of an Euler-Bernouli beam with continuous elasticity and density [17]. Their approach is based on indirectly solving the fourth order governing equation using a system of Fredholm intergral equations.

Their solution insures the validity of a solution to arbitrary axial grading or cross section varying in a buckling problem.

Moreover, Swenson, Jr. performed a simple DC network analysis on non-uniform columns and beams [18]. This analysis was further performed on a stepped column with a variable flexural rigidity as well as a tapered column with varying cross section. Nonetheless, the solution was performed only on pin-pin boundary conditions. Coskun and Attay managed to solve for the buckling load of columns with variable cross sections using a variation iteration method (VIM) [19]. The VIM method proved to be a very powerful method in solving nonlinear partial differential equations, and because the results where efficient and reliable, it remains an important tool in solving such buckling problems as. The downside of this tool is its inability to find the analytical solution for any random variation in flexural rigidity. On the other hand, Oyekoya and El Zafrany studied functionally graded columns using a finite element analysis [20]. They used the element formulation of type Mindlin and Reissner employed to solve for the critical buckling load and to study the finite strain model and smooth fiber distribution. Also, they provided optimum fiber distribution to obtain the maximum buckling load. In a similar context, Zhong and Yu presented a plane elasticity solution for functionally graded beams utilizing the semi inverse method [21]. Such solutions can be utilized as a benchmark for other approximate solutions of similar manner. Similarly, Yilmaz et al. provided a solution for the same problem as Zhong by utilizing a localized differential quadrature method (LDQM) and providing a generalized solution for Eigen value problem governed by fourth order differential equations [22]. Likewise, Chandran and Rajendran provided an exact solution for the same problem using the principle of conservation of energy [23]. Their solution is only limited to an assumed deflection function. In a similar manner, Singh and Li proposed a solution for different FGMs by utilizing Newton's Eigen value iteration method (NEIM) [24]. However, their method indicated the buckling of functionally graded columns occurred for different FGMs such as checkerboard, axially graded columns under free weight, and axially graded column subjected to concentrated loads. The NEIM helps in introducing a low dimensional mathematical model and transcendental Eigen value problems, which can be helpful in different applications for shape optimization. In an attempt to improve previous

models, Huang and Li suggested an approach that includes shear deformations at the circular cross section in the model [25].

Further studies on FGM included Ding et al. solving plane anisotropic functionally graded beams [26]. Also, Shariat and Eslami performed a buckling analysis of functionally graded thick plates under mechanical and thermal loadings [27]. The study compared between the first order and third order shear deformation theory in obtaining buckling load values. The comparison showed that using a 1st order shear deformation theory over predicts the buckling values while a 3rd shear deformation provides precise results. Bagherizadeh et al. studied buckling of FGM cylindrical shells [28]. The findings showed that a critical buckling load of a cylindrical shell is greater under axial pressure than under a lateral or combined pressure load. In additional research, Batra and Li investigated the relationship between the buckling loads of functionally graded Timoshenko element and homogenous Euler-Bernouli beams [29]. Closed form solutions presented a relationship between the Timoshenko, Euler-Bernouli beams, and homogenous Euler-Bernouli beams for simply supported, clamped, and clamped-free beams. The closed form solution defined aided in deriving an eigenvalue problem to determine the critical buckling load of an FGM Timoshenko beam. The relationship between the different beams displays a solution to buckling of FGM Timoshenko beams by using an equivalent homogenous Euler-Bernouli beam with two additional constants that are dependent on the young modulus and Poisson ratio. Kadoli et al. studied the effect of power law exponent of metal ceramic FGMs [30]. Outcomes of studying the static behavior of metal ceramic FGMS for different power laws showed that deflections, stresses, and location of neutral surfaces are highly dependent on power law index. On the same subject, Heydari found exact solutions for FGM beams with rectangular and annular cross-sections [31]. Main outcomes presented revealed the dimensionless mode shapes for a specific buckling load is independent of the material used .

Despite the fact that researchers conducted studies on the buckling of inhomogeneous materials, in only a few cases did the researchers concern themselves with the buckling of checkerboard and FGM columns. The current study focuses on two aspects. First, it determines the buckling load of checkerboards columns, investigates the effects of phase contrast on the buckling capacity, and identifies the microstructures that provide the highest and lowest buckling mode. Second, it focuses

on investigating the FGMs that enhance the buckling capacity, identifies the young modulus parameter change on the buckling capacity, and presents the relationship between mode shapes and FGMs.

Chapter 3. Buckling of Checkerboard Columns

3.1 Introduction

This chapter presents a new study that investigates the buckling capacity of inhomogeneous columns with two-phase checkerboard microstructures at arbitrary phase contrasts and volume fractions. To the best of our knowledge, the buckling of such two-phase checkerboard columns has not been investigated in the past. The microstructure of this column is made up of two materials with very different elastic moduli. A Monte Carlo technique is used to generate checkerboard microstructures at arbitrary phase contrasts, volume fractions, and the spatial distributions of the phases. After generating the microstructure, the eigenvalue problem is then solved numerically using a linear perturbation analysis that is implemented in the commercial finite element software ABAQUS [31]. This procedure is repeated for all microstructural realizations with the following objectives−being investigated, i) determine the critical buckling load for checkerboard columns as a function of the volume fraction; ii) study the effect of phase contrast on the critical buckling load; iii) identify the microstructural realizations (spatial distribution of individual phases) that result in achieving the highest and the lowest buckling loads for a given volume fraction.

3.2 Problem Formulation

3.2.1. General Buckling Equation

The governing equation for the buckling of an inhomogeneous long column is provided by the following equation:

$$E(x)I\frac{\partial^2 v}{\partial^2 x} + P_{cr}v = 0, \tag{1}$$

where $E(x)$ indicates the spatial dependence of the modulus of elasticity, I represents the area moment of inertia, v is the transverse deflection, and P_{cr} is the critical buckling load. It is well-known that for a homogeneous column with $E(x) = E$, the critical buckling load is given by $P_{cr} = \frac{C\pi^2 EI}{L^2}$. Here, C is a constant representing the type of boundary condition and L is the column length.

In the present study, the microstructure is a two-phase material with a random checkerboard microstructure. Such a random checkerboard can be seen as a set of deterministic checkerboards: $B = \{B(\omega); \omega \in \Omega\}$ (see [32]). Here, Ω is the realization space and ω is the specific microstructural realization under consideration. For a two-phase checkerboard column with phases 1 and 2, $(B(\omega) = B_1 \cup B_2)$, with the local modulus of elasticity given by E_1 and E_2, respectively. Mathematically, the microstructure can be defined completely using the indicator function defined as [32]:

$$\chi_1(\vec{x}, \omega) = \begin{cases} 1 & if \ \vec{x} \in B_1 \\ 0 & f \ \vec{x} \in B_2 \end{cases} \tag{2}$$

Using Eq. (2), the local modulus of elasticity at any point in the column can be identified as follows:

$$E(\vec{x}, \omega) = \chi_1(\vec{x}, \omega)E_1 + [1 - \chi_1(\vec{x}, \omega)]E_2, \tag{3}$$

where $\vec{x}$ is a position vector, and E_1 and E_2 are the modulus of elasticity of the individual phases. The volume fraction of phase 1 can be simply recovered by the ensemble averaging of the indicator function

$$\alpha = \langle \chi_1 \rangle \tag{4}$$

Due to the randomness in the modulus of elasticity [as seen in Eq. (3)], it is difficult to find an explicit closed-form analytical solution for Eq. (1). Thus, in this study we used Monte Carlo runs along with finite element analysis to solve Eq. (1) and to obtain the critical buckling load.

3.2.2. Finite Element Modeling using Linear Perturbation Analysis

As mentioned previously, a Monte Carlo technique is employed in order to generate checkerboard microstructures at arbitrary phase contrasts, volume fractions, and the spatial distributions of the phases. After generating the microstructure, the eigenvalue problem is then solved numerically using linear perturbation analysis with the finite element software ABAQUS; this is due to its versatility in handling such problems. A linear perturbation analysis step provides the linear response of the system at the base state, and utilizes estimating elastic buckling by the use of eigenvalue extraction. Eigenvalue buckling is generally used to approximate the

critical buckling loads of stiff structures. Usually the loading on stiff structures is either an axial or membrane loading. The response to such loading involves small deformation before buckling. A simple example of a stiff structure is the Euler column, which responds firmly to a compressive axial load until a critical load is reached, when it bends suddenly and exhibits a much lower stiffness. However, estimation using general eigenvalue extraction is useful especially if the perturbation loads are elastic before the buckling occurs. The eigenvalue solution is obtained by making the model stiffness matrix singular. The model matrix is then described by $K^{ij}v^i = 0$ where K^{ij} is the tangent stiffness matrix and v^i is the displacement matrix [33].

In the proposed study, a circular cross-section column with a diameter of 50 mm and length of 4000 mm was used for the proposed analysis (see Figure 3.1). The dimensions were chosen so as to make sure elastic buckling is always ensured. Pinned connections were considered for both ends. The column is modeled with different material configurations for each simulation using deformable Timoshenko beam elements coded as B21 in ABAQUS. This type of line element accounts for the transverse shear stress. This happens because as shown with Shnabl and Planinc [34] the transverse shear stress does affect the critical buckling load. Also, as it provides better results for slender beam, the B21 element is relevant to the current study [33]. As for the boundary condition used in the FE modeling, the pin-pin connection was modeled by stopping the deformation in the axial and transverse directions for the bottom end. The restriction of deformation was only applied on the transverse direction for the top end to allow loading in the axial direction.
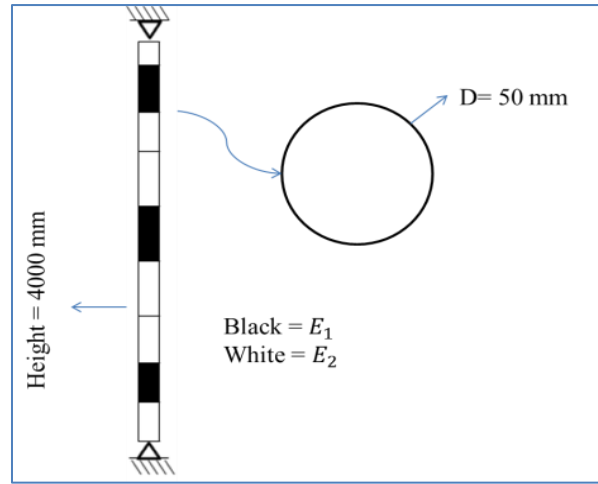
Fig 3.1: Two-phase checkerboard column with circular cross section

3.3   Materials combinations

In each analysis step, the column consists of two materials with different elastic modulus (E). The choice of the two materials used is based on the contrast, which is the ratio between the largest and the lowest elastic modulii, and can be calculated using the following equation:

$$k = \frac{E_1}{E_2} \tag{5}$$

Table 3.1 presents the material combinations considered in the present study. The choice of materials is based purely on providing different levels of contrast varying from very low to very high ratios. Columns made of steel and wood have the highest contrast while columns made of aluminum and copper hold the lowest contrast. The other two conditions have almost equal contrasts. The use of a similar contrast helps in identifying behavioral similarities of the material combinations.

Table 3.1: Material combinations

Material 1	Material 2	E_1(GPa)	E_2(GPa)	k
Steel	Magnesium	200	45	4.44
Steel	Wood	200	11	18.2
Magnesium	Wood	45	11	4.1
Copper	Aluminum	168	69	2.43

3.4   Methodology

For each analysis realization, the column is discretized into 100 segments, and each segment is assigned a random combination of E_1 and E_2. The volume fraction will be changed by increasing the fraction of the E_1 gradually from 0 to 100%. The numerical simulations are performed 500 times for each volume fraction to account for material randomness. Table 3.2 summarizes the contrast, volume fractions, and the number of realizations employed in the numerical simulations. In all, over 18,000 runs were conducted in order to determine the critical buckling load and to identify the microstructural realizations (spatial distribution of individual phases) resulting in the highest and lowest buckling loads for each volume fraction.

Figure 3.2 highlights the methodology employed in the current study. In step (a), a particular realization of the checkerboard is sampled randomly and its finite element model is set up in ABAQUS. The pin-pin boundary conditions are then applied at the column ends. Next, in step (b), a concentrated unit load was applied and the eigenvalue problem was solved in order to obtain the mode one critical buckling load and the corresponding mode shape. The procedure was repeated over 18,000 times in order to cover the entire realization space highlighted in Table 3.2. Subsequently in step (c), the results were compiled to determine the minimum, maximum, and ensemble averaged buckling load for each volume fraction and contrast. In addition, the spatial distributions of the phases corresponding to the maximum and minimum buckling load were determined to identify the microstructure that corresponds to the best and worst designs, respectively. Finally, a statistical analysis of the results was performed in order to obtain various statistical moments such as coefficient of variation, skewness, and kurtosis.

		Volume fraction (in percentage)									
		10	20	30	40	50	60	70	80	90	
Contrast (*k*)	2.43	500	500	500	500	500	500	500	500	500	Total runs = 18,000
	4.1	500	500	500	500	500	500	500	500	500	
	4.4	500	500	500	500	500	500	500	500	500	
	18.2	500	500	500	500	500	500	500	500	500	

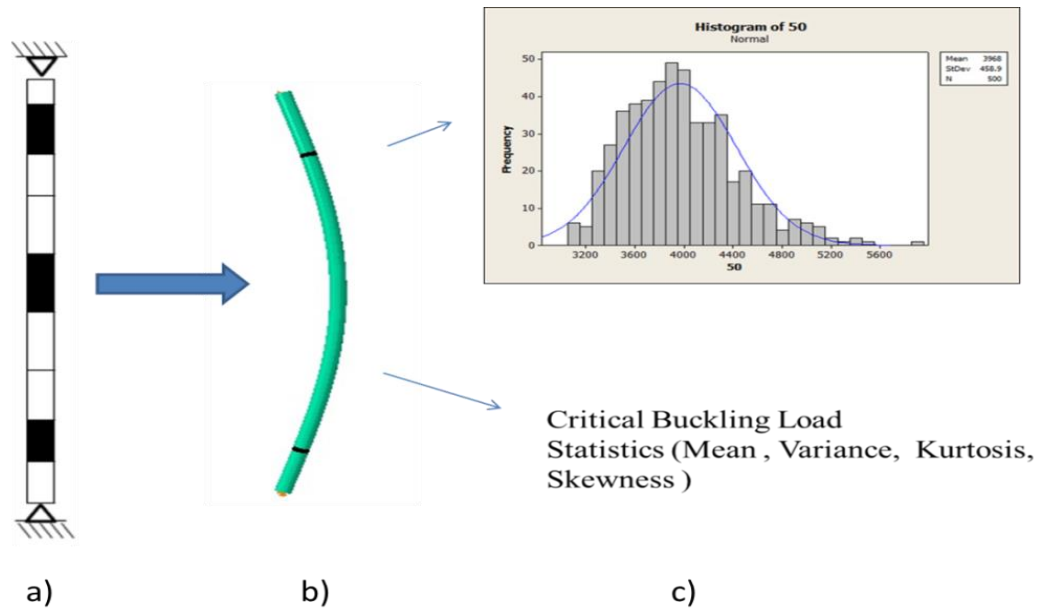Table 3.2: Number of runs and the total realization space

Fig 3.2: Methodology employed: a) Microstructure of the column; b) Buckling mode shape; c) Statistical moments

Figure 3.3 displays the methodology used in generating random checkerboards for the sake of the study. The thesis utilized Matlab to generate the input files and ran them through Abaqus. The output results are then imported to Matlab and analyzed using the software.
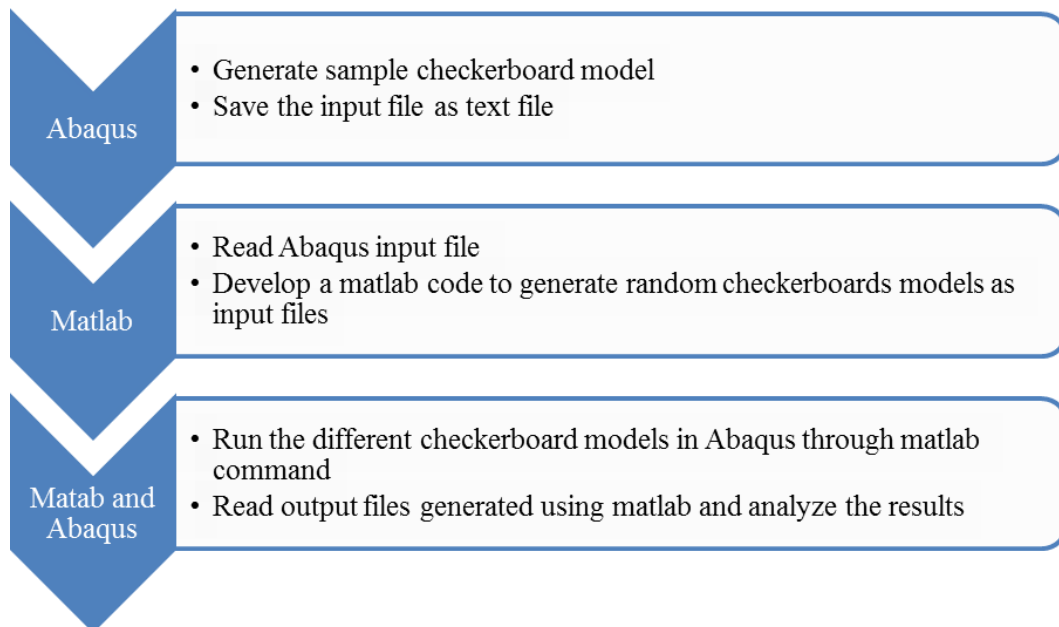

Fig 3.3: Methodology used in checkerboard study

3.5 Results

3.5.1. Critical buckling load of the checkerboard column as a function of the volume fraction

Prior to a discussion on the numerical results, it is important to define a rescaled buckling load as follows:

$$P_c = \frac{P_{cr}L^2}{\pi^2 I} \tag{6}$$

where P_{cr} is the numerically obtained mode in one critical buckling load and P_c is the rescaled buckling load (typically in GPa). An alternative interpretation of P_c would be the equivalent effective elastic modulus of the checkerboard column. Depending upon the context, P_c could represent either the mean, minimum, or maximum rescaled buckling load.

Figure 3.4a, presents the rescaled buckling load (average, maximum, and minimum) for a checkerboard column made up of steel and wood. The modulus of elasticity for wood is 11 GPa and for steel is 200 GPa; therefore, the contrast of the microstructure is k=18.2. It is evident from this figure that the lower modulus material (wood) affects the rescaled buckling load significantly more than the material with a higher modulus (steel). Even at a 50% volume fraction, the average value of the rescaled buckling load is only about 20.85 GPa. Similarly, the rescaled buckling load (average, maximum, and minimum) for checkerboard columns made up of steel and magnesium (k=4.44) and magnesium and wood (k=4.1) are plotted in Figures 3.4b and 3.3c, respectively. The material properties for this individual phase are provided in Table 1. It is evident from these plots that as the volume fraction of the stiffer material increases, the rescaled buckling capacity of the column increases. At a volume fraction of 50%, the rescaled buckling loads are 73.46 GPa and 17.68 GPa, respectively. Further, it can be noted that the trends for the average, minimum, and maximum rescaled buckling loads are identical for microstructures with similar contrasts. Finally, the rescaled buckling load (average, minimum, and maximum) for ductile iron and aluminum is plotted in Figure 3.4d. This particular microstructure has a contrast of 2.43.
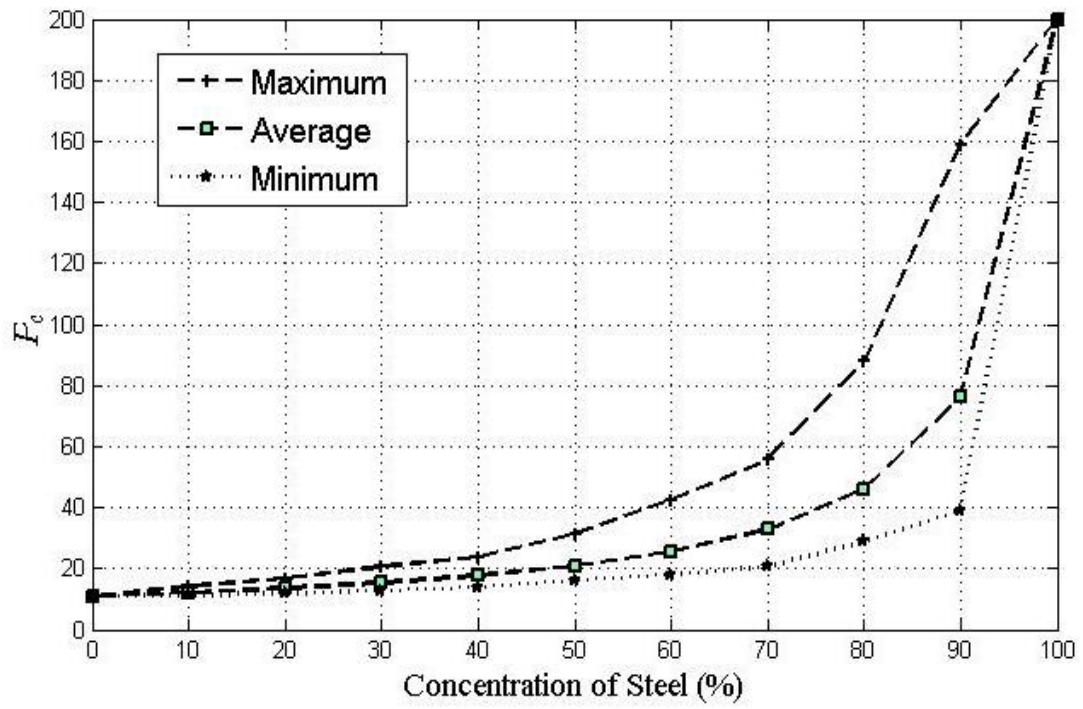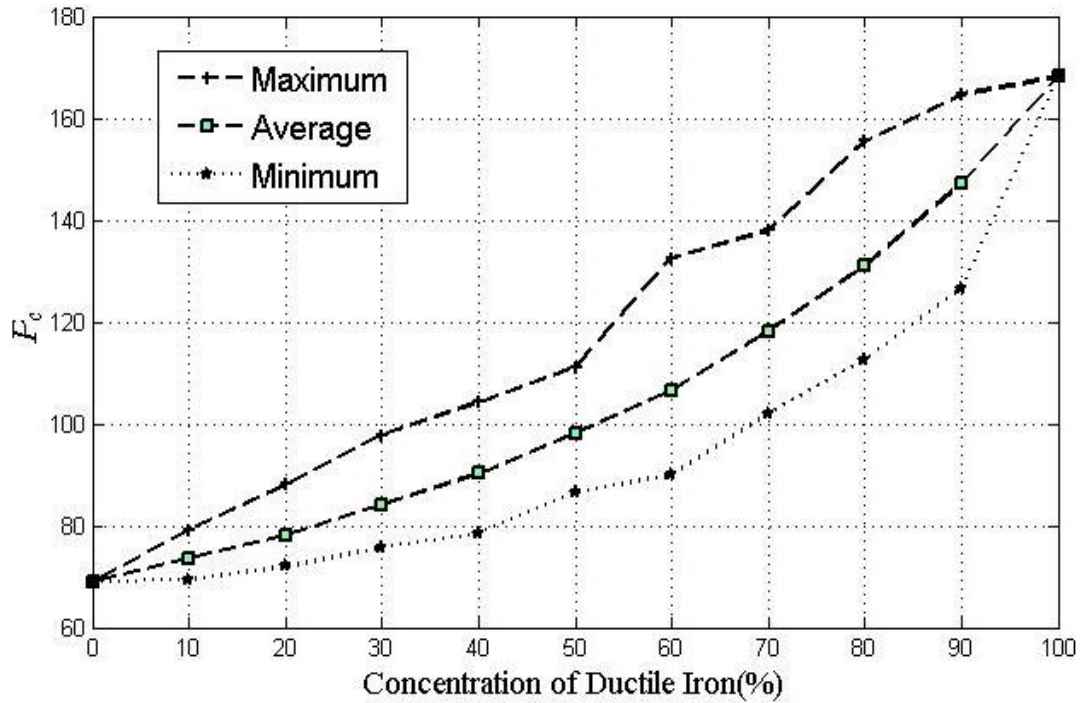
(a)
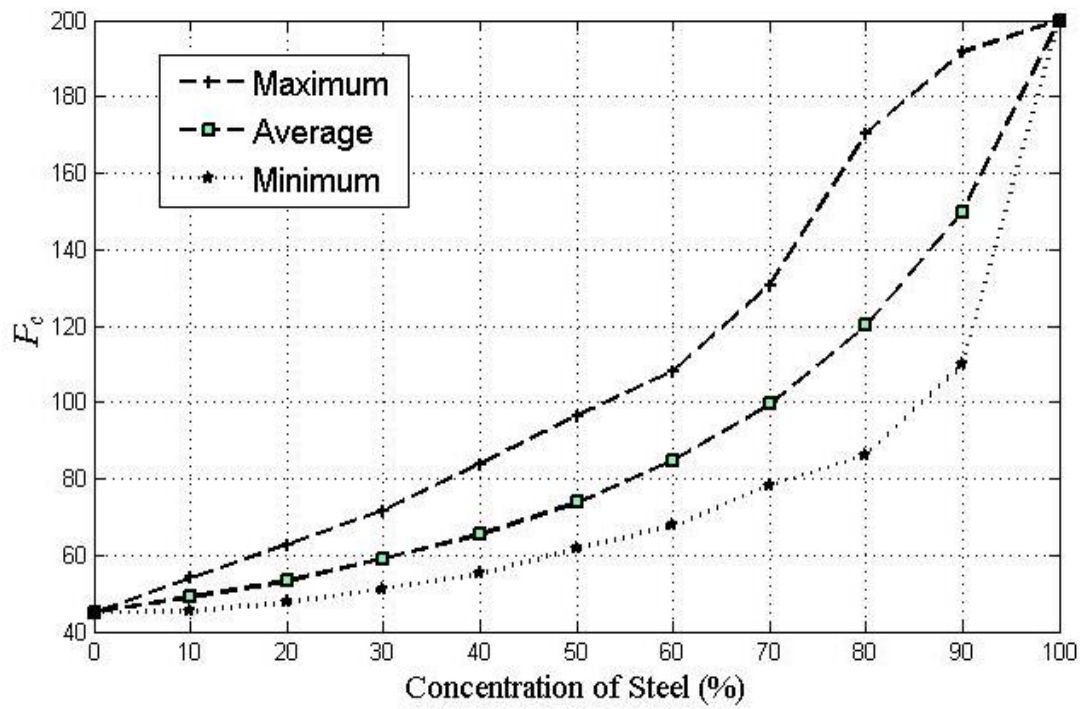
(b)
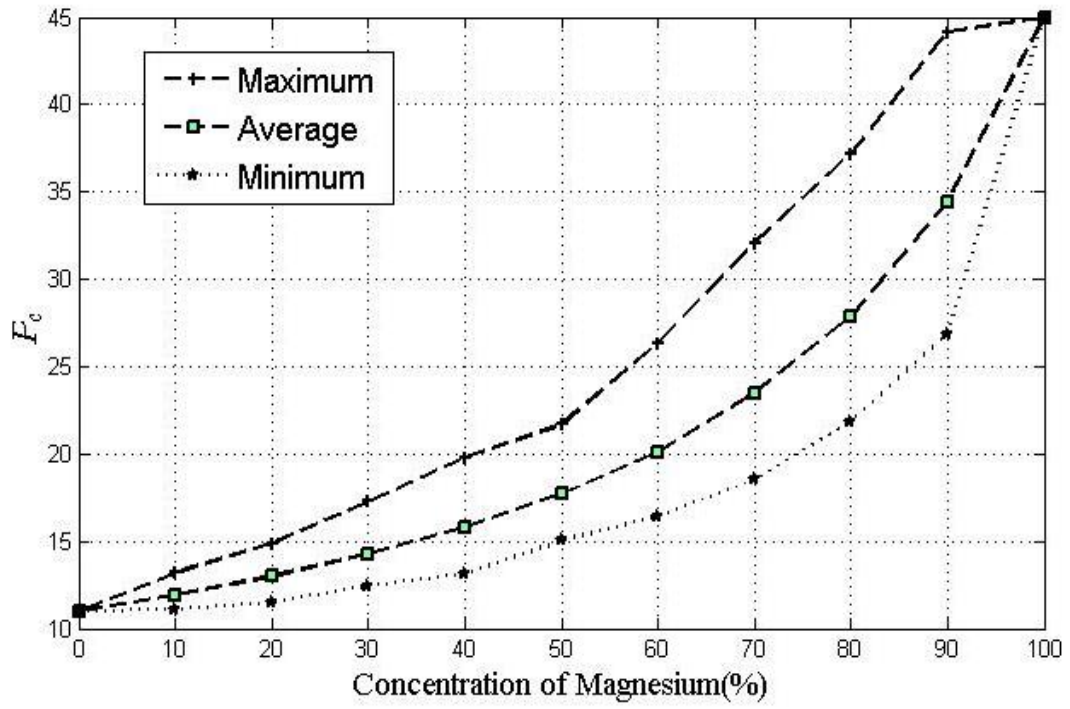
(c)

(d)

Fig .3.4: Rescaled buckling load (average, maximum, and minimum) as a function of the volume fraction: a) steel and wood microstructure (k=18.2); b) steel and magnesium microstructure (k=4.44); c) magnesium and wood microstructure (k=4.1); d) ductile iron and aluminum (k=2.43).

Based on the numerical results obtained, it is possible to infer the analytical form for the average value of the rescaled buckling load as well as the ensemble averaged critical buckling load as given in the equations below.

$$\langle P_c \rangle = \left[\frac{E_1 E_2}{\alpha E_2 + (1-\alpha)E_1} \right] \quad \text{(Rescaled ensemble averaged buckling load)} \quad (7a)$$

$$\langle P_{cr} \rangle = \frac{\pi^2 I}{L^2} \left[\frac{E_1 E_2}{\alpha E_2 + (1-\alpha)E_1} \right] \quad \text{(Ensemble averaged buckling load)} \quad (7b)$$

In the above, E_1 and E_2 are the individual phase elastic moduli, α is the volume fraction of the phase 1 and the operator $\langle \bullet \rangle$ indicates the ensemble averaging.

3.5.2. Effect of phase contrast on critical buckling load

In order to clearly understand the effect of the phase contrast, the notion of normalized buckling load is introduced. This is obtained by normalizing the maximum and minimum buckling load for each material in combination with the ensemble averaged buckling load for the given combination.

$$P_n = \frac{P_{cr}}{\langle P_{cr} \rangle} \quad (8)$$

In Figure 3.5a, the normalized buckling load is plotted as a function of contrast and volume fraction of the stiffer phase. When the volume fraction is 0 or 100%, all the curves converge to $P_n = 1$. This is because the microstructure is essentially homogeneous at these volume fractions. It is also evident from this plot that with an increasing contrast the curves for maximum and minimum normalized buckling loads are farther apart. Furthermore, from Figure 3.5b, it is evident these curves are identical when the contrasts are similar. Based on these observations, one can postulate the following functional form for the normalized buckling load

$$P_n = f(\alpha, k) \tag{9}$$
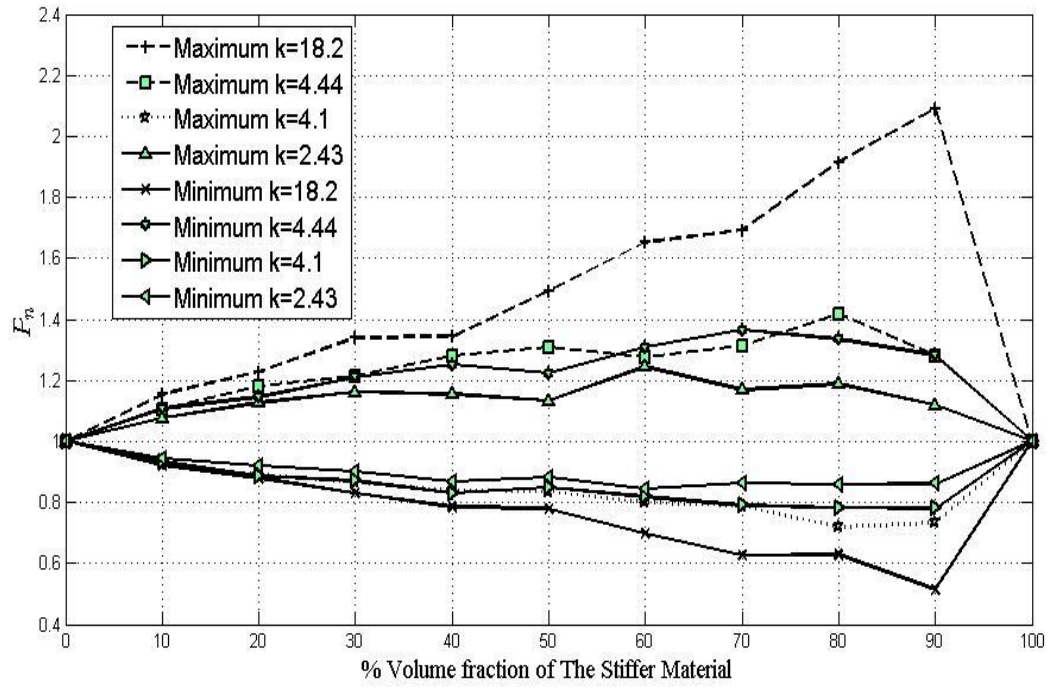
(a)
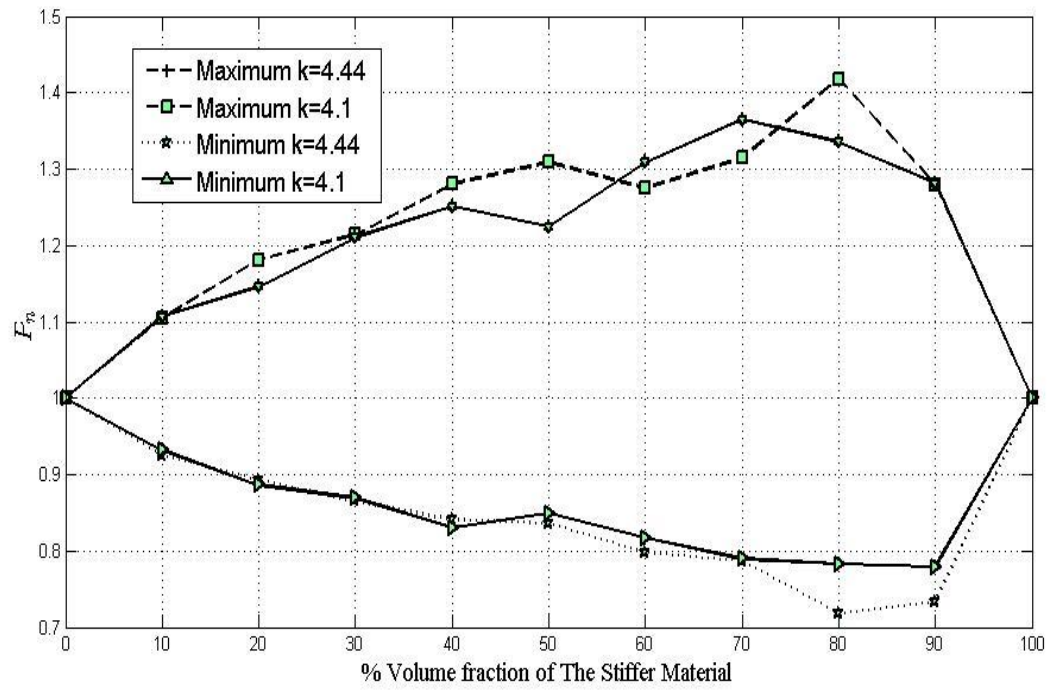
(b)

Fig .3.5: Normalized buckling load (maximum and minimum) as a function of the volume fraction of the stiffer phase: a) differing contrasts; b) similar contrasts.

3.5.3. Spatial distribution of individual phases

In order to determine the spatial distribution of individual phases corresponding to the maximum (best column design) and minimum (worst column design) buckling loads, the corresponding buckling mode shapes are plotted as a function of volume fraction, as shown in Figures 3.6a and 3.6b. The former figure corresponds to a contrast of 2.43 and the later to a contrast of 18.2. From these figures, it is evident that for maximizing the buckling load, it is desirable to distribute the phase with higher stiffness in the middle of the column and vice versa for the minimum buckling load. This essentially implies that by allocating the phase with higher stiffness in the region with higher deflection, the buckling capacity is enhanced.
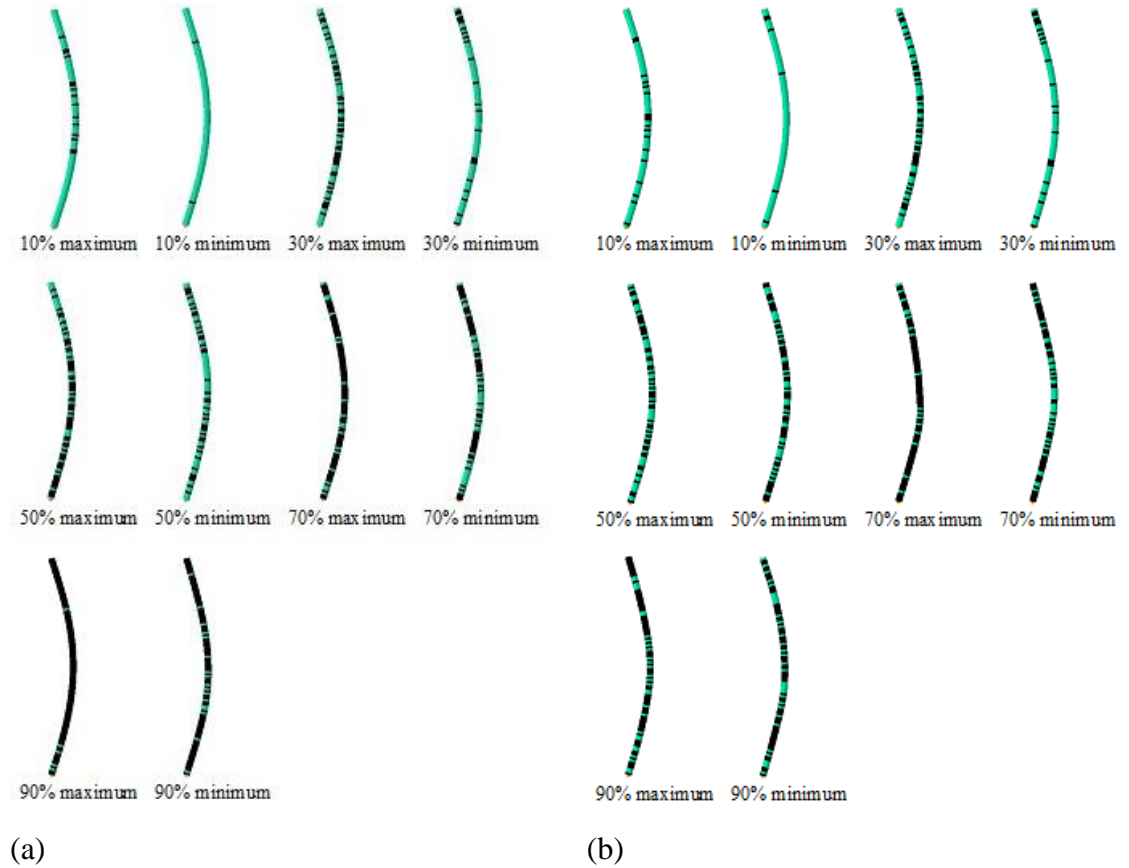

(a)   (b)

Fig 3.6: Buckling mode shapes corresponding to the maximum and minimum buckling load as a function of volume fraction: a) Contrast (k=2.43); and b) Contrast (k=18.2)

3.5.4. Statistical analysis

The numerical simulations performed in this study resulted in 18,000 simulations and the pool of results for the buckling load is best analyzed using statistical tools that include the mean, coefficient of variation, skewness, and kurtosis. The result on the mean value of the buckling load has been extensively discussed in the previous sections. The coefficient of variation for the data set is plotted as a function of contrast and volume fraction in Figure 3.7a. As expected, it is zero when for a homogeneous material that corresponds to 0 or 100% volume fraction. In general, as the contrast increases, the coefficient of variation also increases. It is interesting that the coefficient of variation for the steel-magnesium checkerboard (k=4.44) and that of the magnesium-wood microstructure (k=4.1) are about the same when the magnesium volume fraction is kept the same. In Figure 3.7b, the skewness of the data set is plotted as a function of contrast and volume fraction. By definition, for a perfectly symmetric distribution, skewness is zero. As expected, the skewness is zero at volume fractions of 0 and 100%. In general, it is observed that the skewness is positive for the data set, highlighting that the data set is skewed to the right. Finally, kurtosis (Fig 3.7c) measures the degree to which the data is peaked. By definition, for a normal distribution, kurtosis is zero. Kurtosis is also zero for homogeneous microstructures. It is observed that for the given data, kurtosis is positive indicating relatively a sharp peak for the distribution.
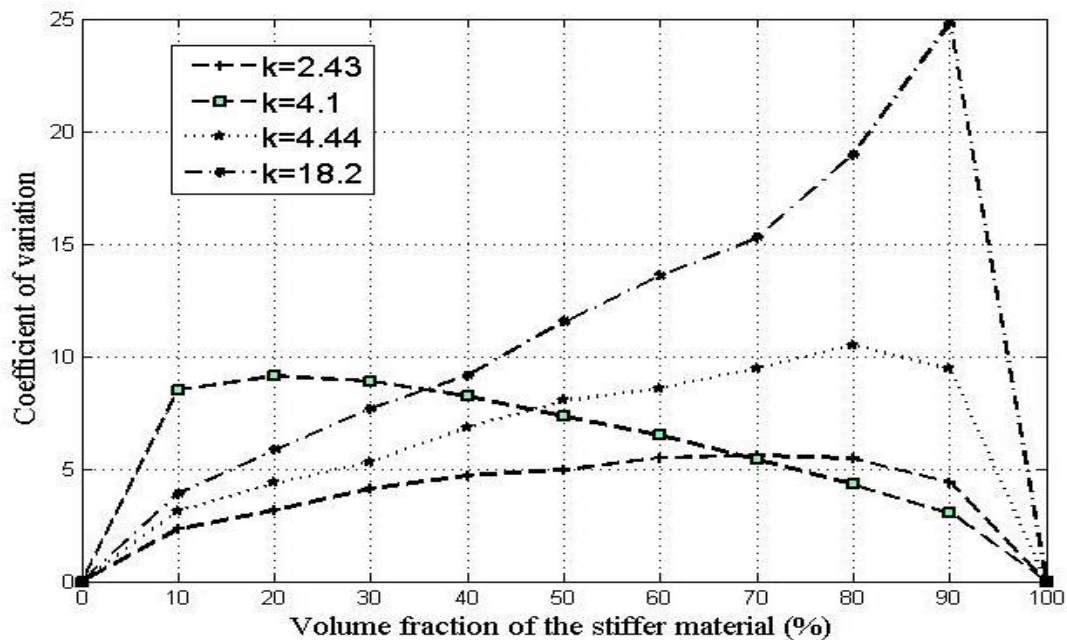
(a)
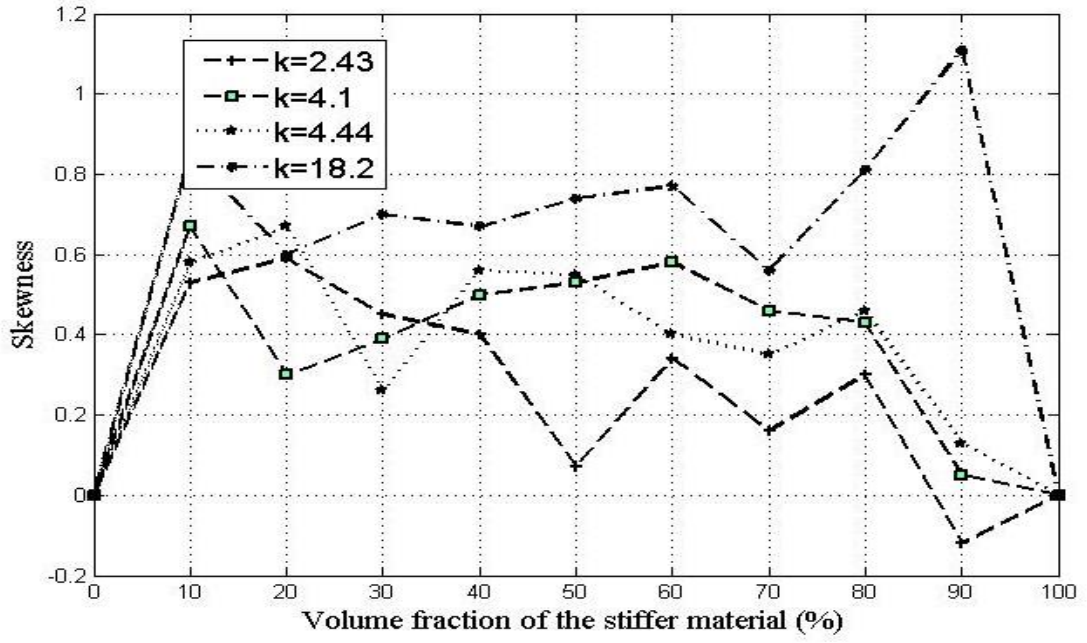
(b)
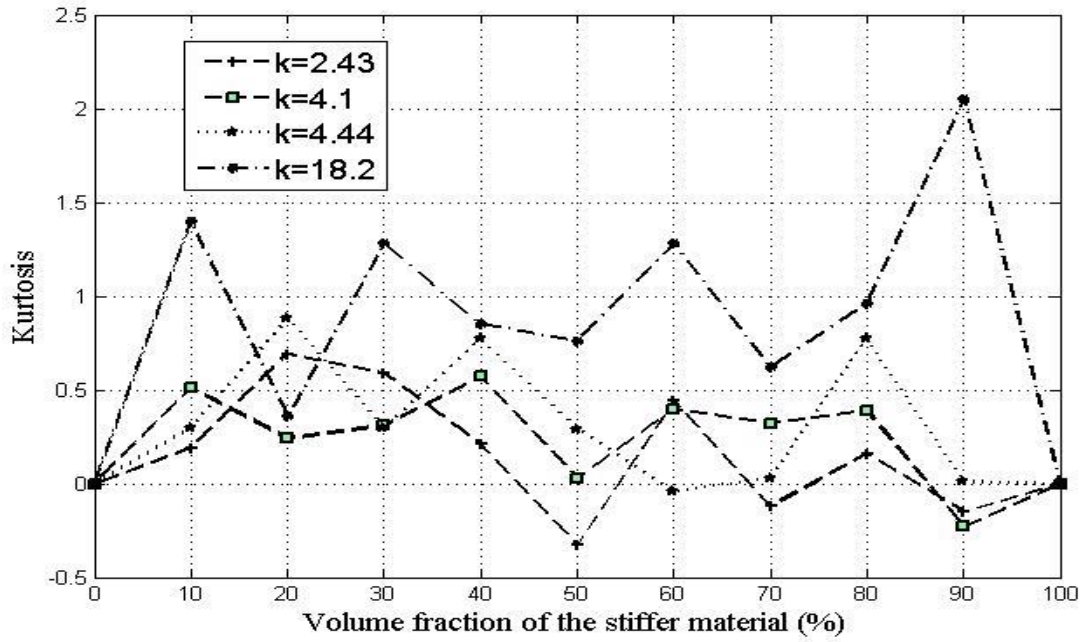
(c)

Fig 3.7: Data statistics: a) Coefficient of Variation; b) Skewness; c) Kurtosis

3.6 Conclusion

In this chapter, a Monte Carlo technique was used to generate checkerboard microstructures at arbitrary phase contrasts, volume fractions, and spatial distributions of the phases. Subsequently, the resulting eigenvalue problems was solved

numerically in ABAQUS by using a linear perturbation analysis. The maximum, average, and minimum values for the critical buckling load were determined and the corresponding buckling mode shapes were identified under pin-pin boundary conditions. It was demonstrated that the ensemble averaged rescaled buckling load $\langle P_c \rangle$ was simply the volume fraction weighted harmonic mean of the individual phase elastic moduli. Also, the normalized buckling load P_n was identical for microstructures with similar contrasts. Furthermore, it was demonstrated that by distributing the phase with higher stiffness in regions of higher deflections (middle), that it then maximizes the buckling capacity of the column and vice versa. Finally, a statistical analysis on the numerical results was conducted by studying the mean, coefficient of variation, skewness, and kurtosis as a function of contrast and volume fraction. To the best of our knowledge, this is the first time an analytical result has been proposed for the critical buckling load of a column with a random checkerboard microstructure.

Chapter 4. Buckling of FGM Columns

4.1   Introduction

This chapter proposes the use of functionally graded material to enhance the buckling capacity of columns. Additionally, the research aims to test different functions for distributing the young modulus; from there it will indicatewhat functions provide the optimal buckling load. The functions utilized will take the form of linear, quadratic, cubic, sinusoidal, and power roles. The common factor between all these functions will be a homogenous column with a young modulus of $150\ GPa$. The homogenous column will be used as a comparison tool to understand the effect of changing the FGMs on the buckling of columns. All of the FGMs will be tested on a column with the same length and end conditions. The FGMs will be solved using two different methods. Firstly, the buckling problem will use the linear perturbation analysis tool implemented in the commercial software ABAQUS. Secondly, the buckling problem will use the Rayleigh-Ritz method. The main objectives of this study are to: i) investigate functions that enhance buckling capacity; ii) define the changes in the buckling capacity as seen in case of changing the homogenous column modulus of elasticity; and iii) present the impact of implementing FGMs on the resulting mode shapes and describe the relation between the FGM distribution and the final mode shape.

The theoretical background for the linear perturbation analysis has been presented in Chapter 3, section 3.2.2, whereas the Rayleigh-Ritz method is briefly explain in the following section.

4.2   Rayleigh Ritz Method (RR)

The RR method, also known as the minimum potential energy method, is extremely useful in obtaining a solution for this type of problem because the deflected shape of the buckling load is unknown and has to be assumed.

The RR method is normally used to obtain the modal frequencies of multi degree freedom systems. The method relies on the minimum potential energy approach, which states that if the potential energy of a conservative structure is minimized, then the admissible function used shows the equilibrium state is stable. In this study, the expression of potential energy is given by [35]

$$\prod = \frac{1}{2}\int_0^L E(x)I\left(\frac{d^2v(x)}{dx^2}\right)^2 dx + \frac{1}{2}\int_0^L P\left(\frac{dv(x)}{dx}\right)^2 dx \qquad (10)$$

where the first term denotes the strain energy while the second term denotes the work potential.

The RR method involved obtains a solution in two simple steps. Firstly, an admissible function satisfies the essential boundary conditions is substituted into the potential energy expression. Secondly, the new potential energy expression is minimized. The desired solution is then obtained by solving the minimized potential energy expression. The solution is then compared with both the literature and the FEM model results. The RR method will be applied on all the different FGMs discussed in the chapter.
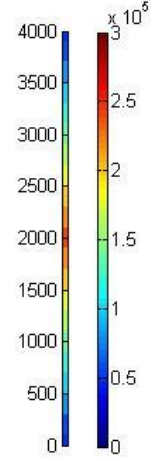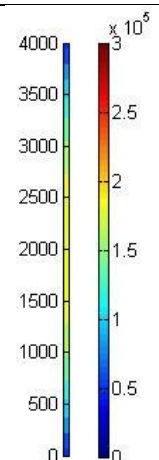
4.3   Methodology

The FGM concept applied throughout the literature is dependent on changing the flexural rigidity $K = E(x)I(x)$ of a certain column. In this paper, The FGM concept applied was only dependent on varying the young modulus along the length while keeping the moment of inertia as a constant value. Different functions were used to distribute the material over the column length. A common factor in developing the different functions used was E_{hom} as defined in Eq.11, which was solved for the different proposed functions. Each function was solved several times with only one variable changing, which is $E(x = 0)$. The introduction of Eq.11 was to produce a common homogenous column for comparison purposes. The main concern regarding this solution was ensuring the symmetry of the function obtained.
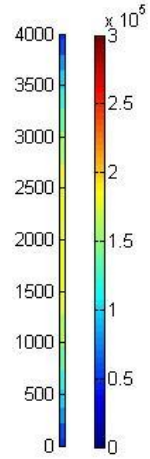
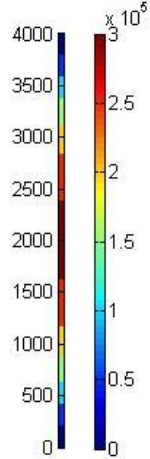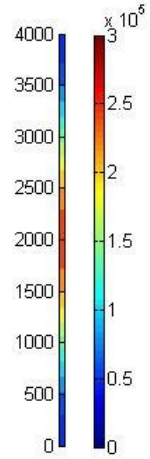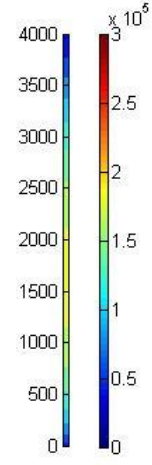$$E_{\text{hom}} = \frac{\int_0^L E(x).dx}{\int_0^L dx} \qquad (11)$$

The second step after obtaining the functions and their parameters will be in solving the differential equations separately using FEM and RR and then comparing their results with the literature. In the FE modeling, the material's modulus of elasticity will be introduced as segments along the length. The column was discretized

into 100 segments and each segment was assigned an increment of E value thereby allowing the function to be depicted as accurately as possible. Table 4.1 displays the different mathematical functions used to distribute the young modulus and represents them graphically. Tables A.1 and A.2 in the appendix provide the function parameters for each mathematical equation used.

Table 4.1: Mathematical and graphical FGM Representations for each function

Function	Mathematical representation	Graphical representation
Bilinear Function	$E(x) = \begin{cases} a + bx & 0 < x < L/2 \\ c + dx & L/2 < x < L \end{cases}$	
Quadratic Function	$E(x) = ax^2 + bx + c$	

Cubic Function	$E(x) = ax^3 + bx^2 + cx + d$	
Sinusoidal Function	$E(x) = a + b\sin(\dfrac{\pi x}{L})$	
Squared Sinusoidal	$E(x) = a + b\left[\sin(\dfrac{\pi x}{L})\right]^2$	

Power Function	$E(x) = c + (axL)^b - (ax)^{2b}$	

As for RR method, an assumed polynomial admissible function was implemented and the order of the polynomial was increased until the solution became stable. Then this order was used to solve for the critical buckling load for each function. An example for the different variations of the functionally graded materials is shown in Fig 4.1.
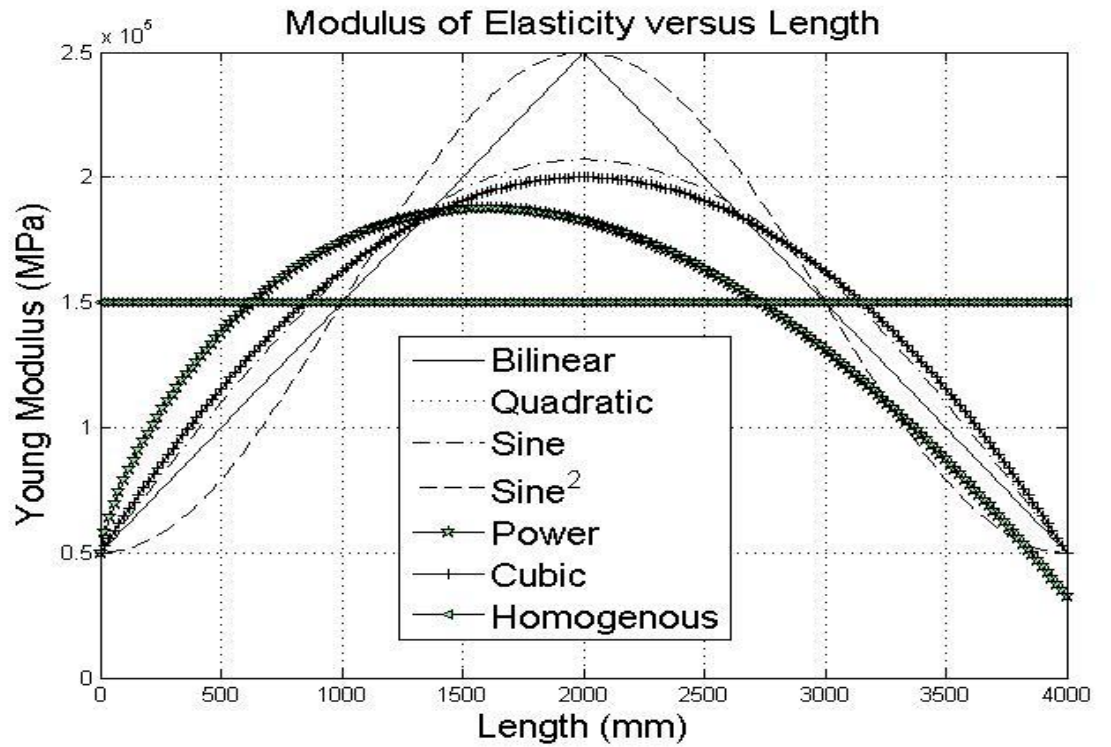
Fig 4.1: FGM distribution for different functions for $E(x=0)$ at $50\,GPa$

4.4   Model Validation

4.4.1.   Validation with examples from the Literature

In order to validate the functionality of both models developed using RR and linear perturbation analysis, similar examples from literature were utilized to verify the accuracy of these models. Elishakoff [13] solved both equations available in Table 4.2 using the RR non-integer power method and RR two-terms solution for a smoothly tapered column. Also, Singh and Li [24] verified their transcendental eigenvalue problem by solving both of the functions in Table 4.2.

Table 4.2: Functions used in literature to distribute the material along the column [13] [24]

Linear	$E(x) = E_0(1 + \dfrac{x}{L})$
Quadratic	$E(x) = E_0(1 - \dfrac{x}{L})^2$

The results obtained for the different models were then compared based on a dimensionless buckling load

$$\overline{P} = \frac{CP_{cr}L^2}{E_0 I} \tag{12}$$

where C denotes the boundary condition factor.

Linear and quadratic functions shown in Table 4.3 were investigated using FEM and RR models. The results obtained indicate the validity of both models as the results were equal with a round off error of 0.0015 (See Table 4.3). These results indicate the possibility to utilize the developed model to further investigate other functions.

Table 4.3: Literature validation

	$\bar{P}$ for Linear	$\bar{P}$ for quadratic
Elishakoff [2]	14.51316	20.8356
Singh and Li [13]	14.5132	20.8356
RR method (current work)	14.5147	20.8356
FEM (current work)	14.5147	20.8356

4.4.2.   Comparison between Linear Perturbation Analysis and the Rayleigh Ritz Method

The validation of FEM model is based on literature aids in trusting the FEM model results. The FEM model results were then used to find the closest admissible function satisfying boundary conditions. The solutions for both the RR method and linear perturbation analysis were then compared in order to obtain linear and quadratic functions (See Figure 4.2, 4.3). The comparison showed that in order to obtain accurate results for the RR method, an admissible high order polynomial function should be used. Other functions were also validated using FEM results to indicate the number of polynomial terms to be used in the admissible function for the RR method (See Table 4.4).
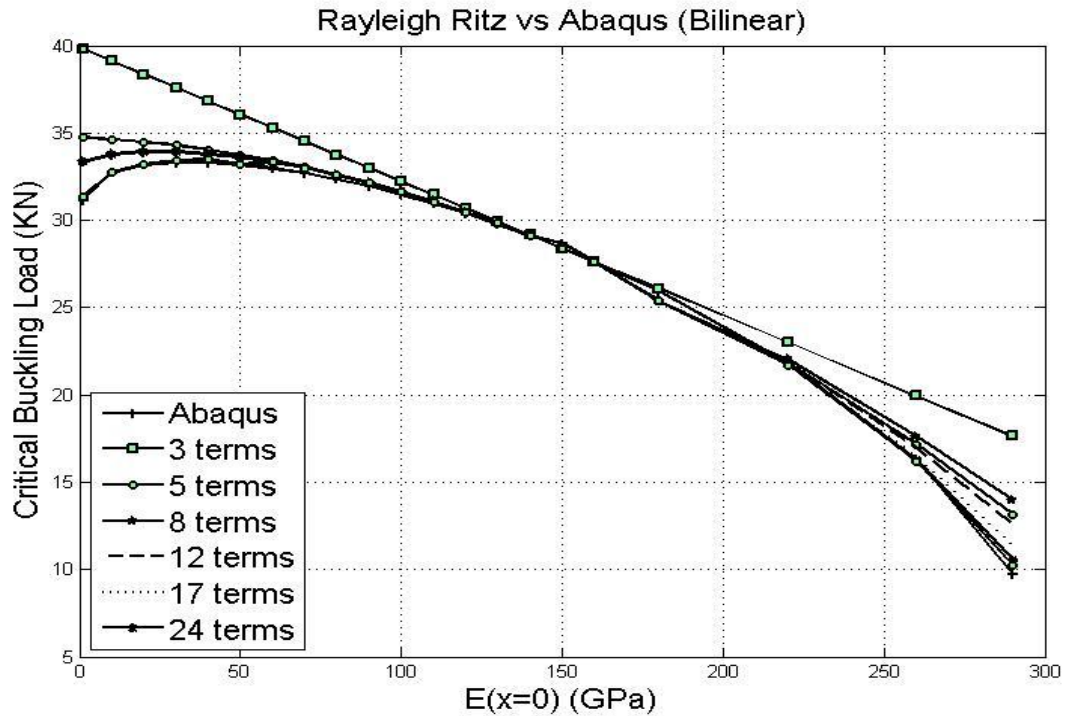
Fig 4.2:Rayleigh-Ritz Vs Perturbation analysis in ABAQUS (Bilinear)
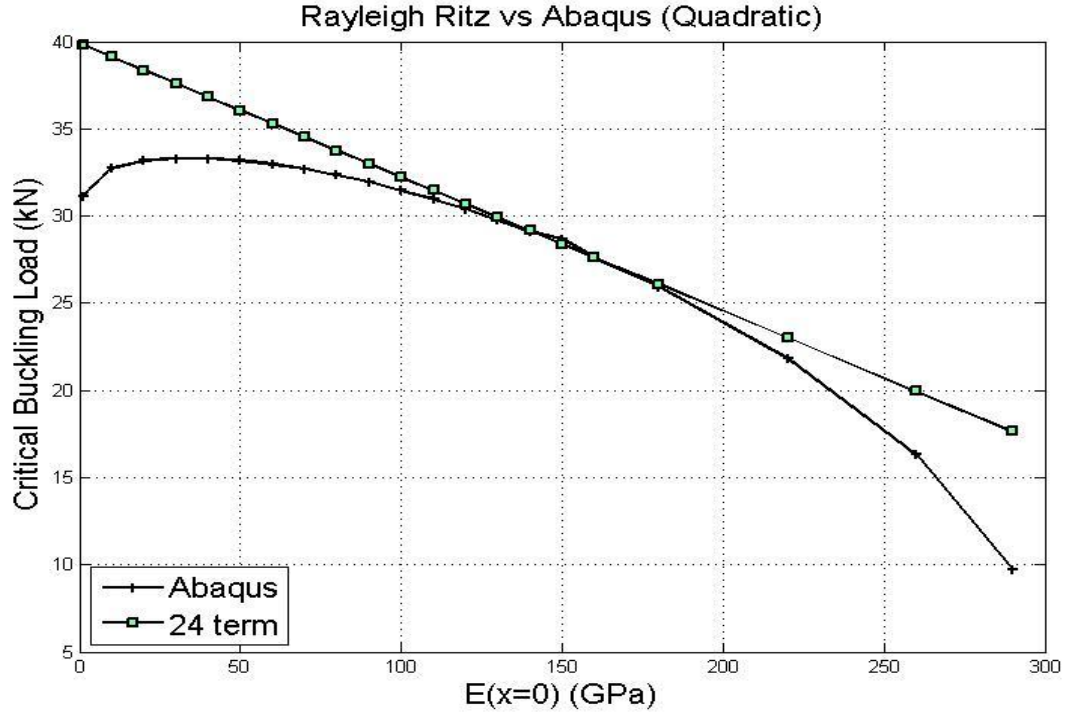
Fig 4.3: Rayleigh-Ritz Vs Perturbation analysis in ABAQUS (Quadratic)

Table 4.4: Number of terms used for RR method

Function	1st order	2nd order	3rd order	Sine	Squared sine	Power
Number of terms	24	24	24	18	15	19

4.5   Results and Discussion

4.5.1. Buckling Capacity

A buckling analysis was performed on various functions with various $E(x = 0)$. The percentage increase in the buckling capacity has been used as a mean of comparison between the different FGM functions and the original critical buckling load of the column. This quantity, R, was calculated using the following equation:

$$R = \frac{P_{in\text{hom}} - P_{\text{hom}}}{P_{\text{hom}}} \times 100 \tag{14}$$

The R values indicate the enhancement of imposing an FGM compared to the homogenous column. Figure (4.4) shows the buckling capacity increase for the

different function is mostly maximum when the $E(x = 0)$ are close to 0 GPa. The cubic order polynomial and sine function provide the maximum increase in the buckling capacity with around 21% increase. An interesting observation was noticed for the squared sine and the 1st order function where the buckling capacity value increases until it reaches a maximum, then it starts decreasing again.
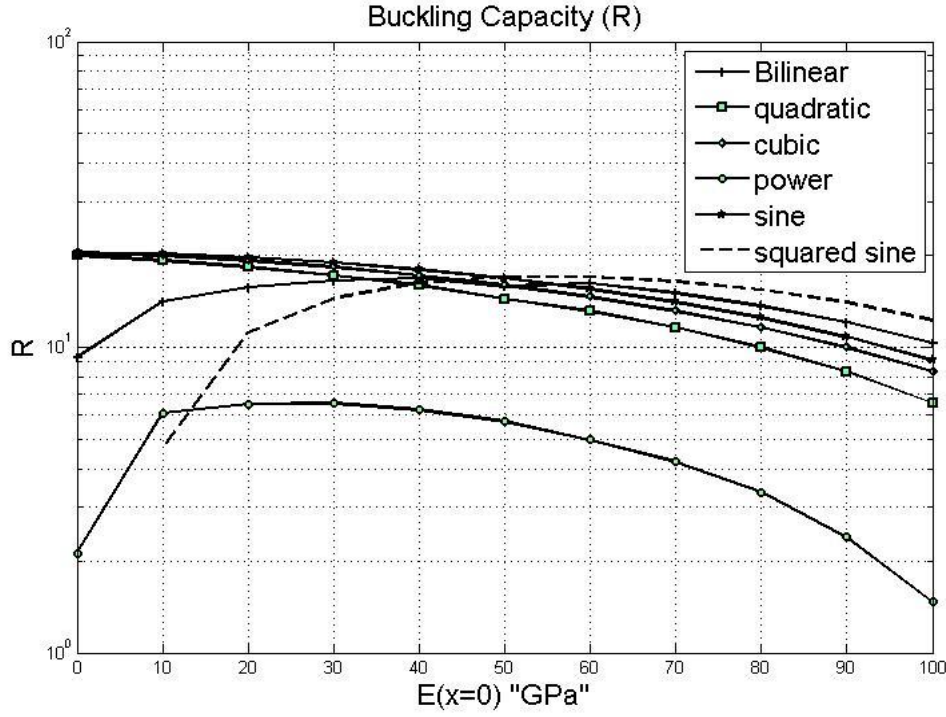
Fig 4.4: Buckling capacity for different functions and $E(x = 0)$

4.5.2. Effect of changing the average value of the elastic modulus

In an attempt to obtain a higher buckling capacity , a 3rd order polynomial produced a maximum buckling capacity at 150 GPa modulus of elasticity was investigated thoroughly to study the impact of increasing or decreasing of the average young modulus. Figure (4.5) shows the maximum buckling capacity obtained for different average modulus of elasticity values varying from 0.5 GPa to 200 GPa. The simulations were all performed for the same end condition of 0 GPa to ensure comparability. As it can be noted from the figure, the buckling capacity is a straight line indicating that changing the average modulus of elasticity has no impact on the buckling capacity increase. This observation indicates the maximum buckling capacity that can be obtained for a pin-pin column with an average E will have a

maximum of 21% increase regardless of changing E and only depending on the shape function of the FGMs.
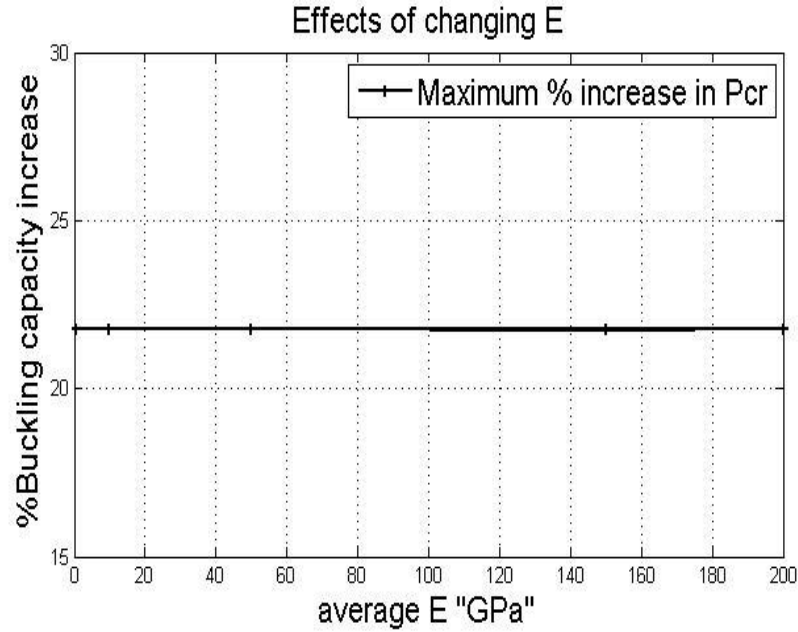
Fig 4.5: Effects of changing average E

4.5.3. Mode shapes

Tables (4.5) and (4.6) display the distribution functions that produced the maximum and minimum buckling loads for different mathematical functions. The tables also pose a critical question on how the FGM distribution can be controlled in order to produce a higher buckling load.

In order to investigate the effects of FGM on mode shapes and the possibility of any given relationship between them, a graph showing mode shape and FGM distribution is constructed. For the sake of comparison, both modulus of elasticity function and mode shape were normalized to obtain a function between 0 and 1.

In Figure (4.6), bilinear functions that produced maximum (E_1) and minimum (E_2) buckling loads and their corresponding mode shapes v are displayed. It is noted from the figure that the FGM producing maximum buckling load is shaped to be close to the mode shape. On the other hand, the FGM that produces minimum buckling load is far from the mode shape.

Table 4.5: FGM distribution functions producing maximum P

Function	$E_{\min}(x)$	$P_{\min}$ (N)
Bilinear	$E_2(x) = \begin{cases} 290000 - 140x & 0 < x < L/2 \\ -270000 + 140x & L/2 < x < L \end{cases}$	9706.3
Quadratic	$E_4(x) = 0.01125x^2 - 45x + 180000$	26588
Cubic	$E_6(x) = -0.01875x^2 + 75x + 10000$	31060.6
Sine	$E_8(x) = 100000 + 157079.6\sin(\dfrac{\pi x}{4000})$	31272.81
$Sine^2$	$E_{10}(x) = 196654.3\left[\sin(\dfrac{\pi x}{4000})\right]^2$	21345.4
Power	$E_{12}(x) = 100000 + (1.191xL)^{0.748} - (1.191x)^{2*0.748}$	29097.14

\

Table 4.6: FGM distribution functions producing minimum P

Function	$E_{\max}(x)$	$P_{\max}$ (N)
Bilinear	$E_1(x) = \begin{cases} 50000 + 100x & 0 < x < L/2 \\ 450000 + -100x & L/2 < x < L \end{cases}$	33493.25
Quadratic	$E_3(x) = -0.525x^2 + 210x + 10000$	34408.65
Cubic	$E_5(x) = -0.05625x^2 + 225x,$	34512.6
Sine	$E_7(x) = 314159.3\sin(\dfrac{\pi x}{4000})$	34451.83
$Sine^2$	$E_9(x) = 70000 + 104882.3\left[\sin(\dfrac{\pi x}{4000})\right]^2$	33555.6
Power	$E_{11}(x) = 40000 + (1.15xL)^{0.7978} - (1.15x)^{2*0.7978}$	30558.5

As for Figure (4.7), the quadratic function that produced maximum (E_3) and minimum (E_4) buckling loads and their corresponding mode shapes v are displayed. It can be noted that the FGM producing maximum buckling load is distributed similar to the mode shape. In contrast the relation between E_4 and $v(E_4)$ is inversed.
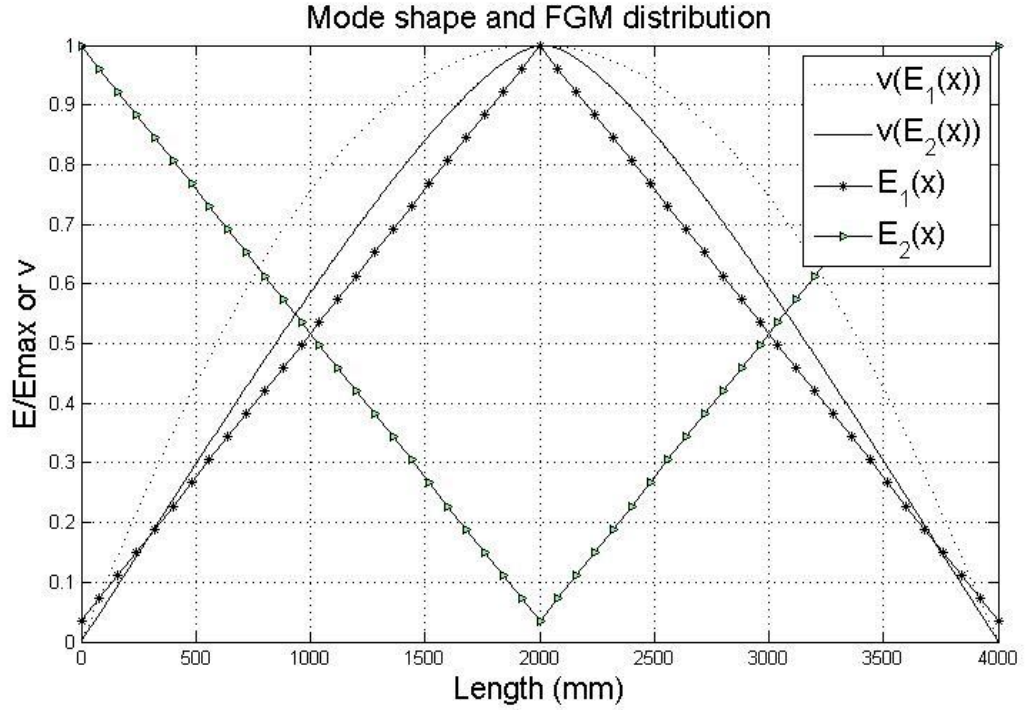
Fig 4.6: Effects of material distribution on buckling mode $E_1, E_2, v(E_1), v(E_2)$

In attempt to further emphasize the relationship between FGM and the mode shape, Figure (4.8) displays both E_5 and E_7 and their corresponding mode shapes $v(E_5)$ and $v(E_7)$. Functions E_5 and E_7 produced the maximum buckling load and this relationship sets a trend. This trend indicates distributing the FGM to fit the mode shape will produce a maximum buckling load for a given column.
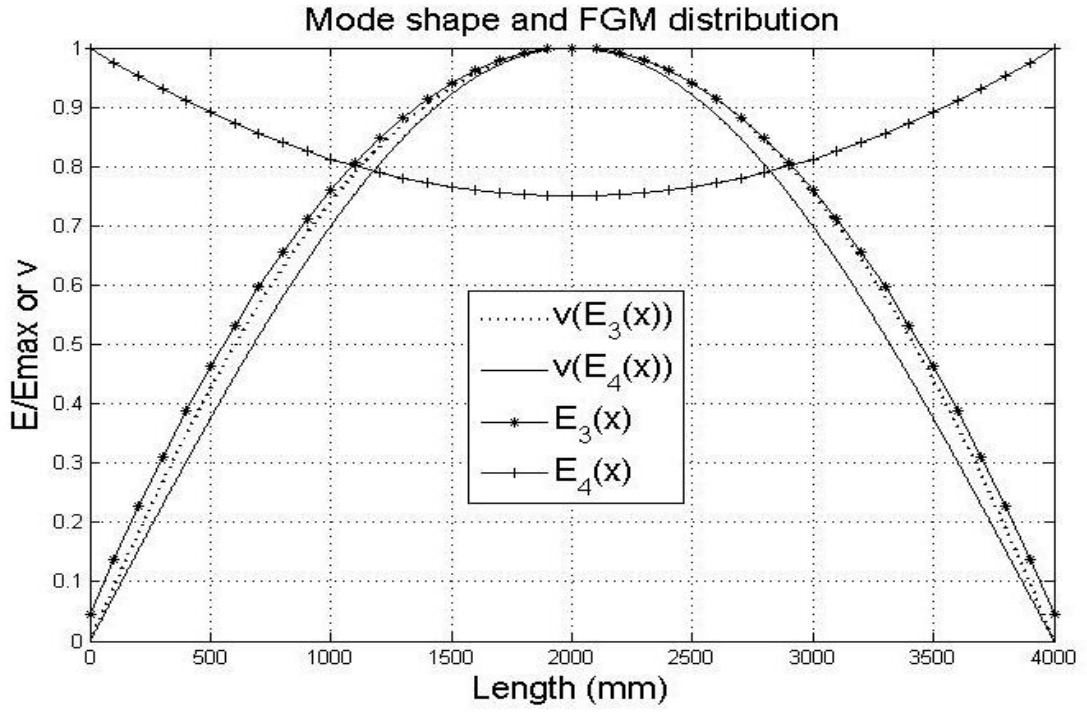
Fig 4.7: Effects of material distribution on buckling mode $E_3, E_4, v(E_3), v(E_4)$
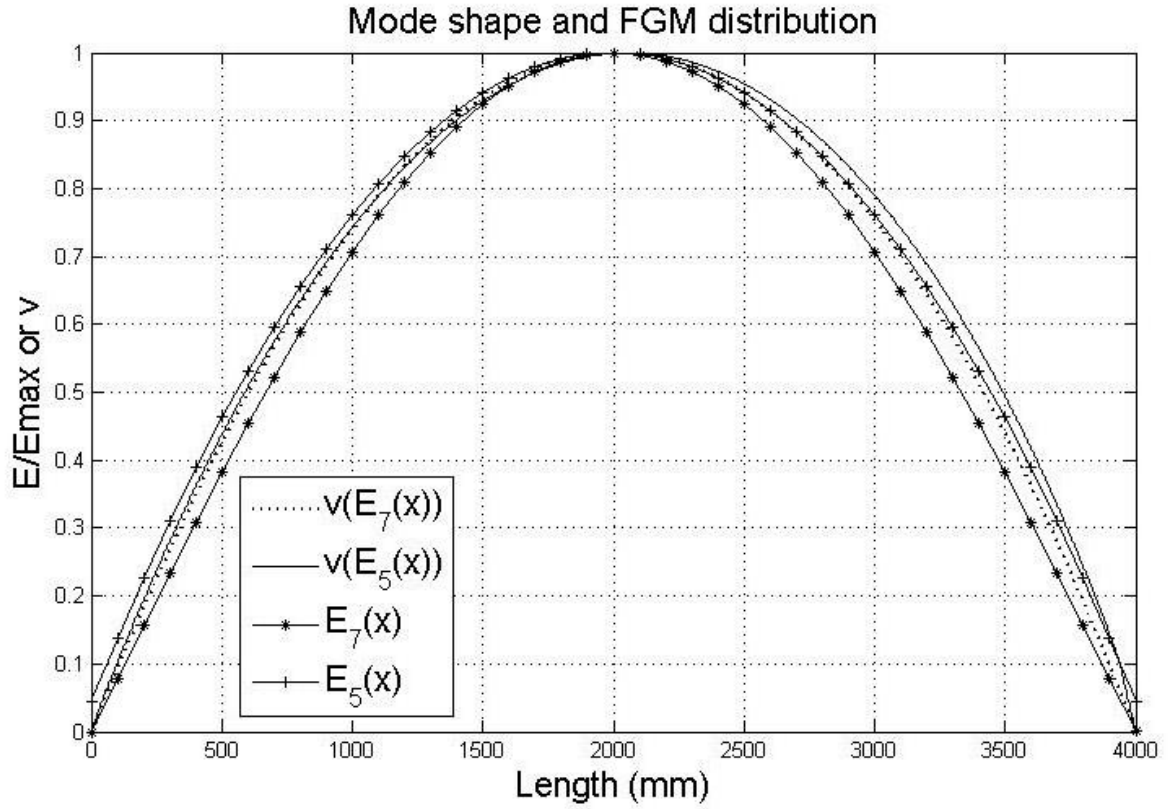
Fig 4.8: Effects of material distribution on buckling mode $E_5, E_7, v(E_5), v(E_7)$

4.6   Conclusion

In this chapter, different distribution functions of FGM columns were studied. The buckling analysis was conducted using linear perturbation via ABAQUS and the Rayleigh-Ritz minimum potential energy approach. Buckling loads and their corresponding mode shapes were obtained for different FGMs for a column with a circular cross-section and pin-pin boundary conditions. It was shown that the sine and the cubic function produced the maximum buckling load with about 21% buckling capacity increase. Also, it was demonstrated that the change in the modulus of elasticity for the basic homogenous column has no effect on the buckling capacity. Finally, it was demonstrated that in order to optimize the column, the FGM should be distributed to fit the corresponding mode shape and this is why a normal sine function and a cubic function produced higher buckling capacity than other functions.

Chapter 5.Summary and Future Work

Inhomogeneous materials are considered as a new emerging field of interest in structural and biological applications. This thesis presents studies of buckling capacity of inhomogeneous materials for checkerboard or functionally graded materials. Firstly, The Monte Carlo technique was used to arbitrary generate different microstructural checkerboard columns. These columns presented an eigenvalue problem that was solved using a linear perturbation analysis implemented in ABAQUS software. The results included maximum, average, and minimum values for critical buckling loads for different microstructures and their relative mode shapes. The ensemble averaged rescaled buckling load was simply the volume fraction weighted harmonic mean of the individual phase elastic moduli. Additionally, microstructures with similar contrast have shown a similar normalized buckling load. As for the mode shapes, it has been demonstrated that by distributing the phase with higher stiffness in an area of maximum deflection provides a maximum buckling load and vice versa. Also, an additional statistical analysis of the realizations was done providing the mean and coefficient of variation for the sample studied.

Secondly, columns with different functionally graded materials were analyzed. The functionally graded materials imposed on the column were generated to have an equivalent average young modulus to a homogenous column with a Young modulus of 150 GPa. The introduction of FGM presents an eigenvalue problem, which was solved using both a linear perturbation analysis and the Rayleigh Ritz method. This was verified with results from the literature. The analysis showed that for a pin-ended column, a maximum buckling load was achieved when either a sine or a cubic distribution FGM was used. Both sine and cubic distribution had an overall increase in buckling capacity of 21%. It was also noticed that changing the equivalent homogenous column Young's modulus has no impact on the buckling capacity improvement. Finally, it was observed in order to optimize the column against buckling, the FGM distribution should match the mode shape in a way where the normalized stiffness will be exactly fitting the unity mode shape.

To the extent of our knowledge, this thesis presented a basic analysis of checkerboard column that was not studied before. Moreover, the study provided an in-depth analysis of FGM impact on buckling. Future work needs to be done to further

investigate inhomogeneous materials effects on buckling. Firstly, studies regarding the non-linear buckling of both checkerboard and FGMs should be conducted because it provides more accurate results and accounts for materials and geometric non-linearities. Additional research regarding the buckling capacity should be conducted to investigate the reason why the maximum buckling capacity is limited to a 21% increase for pin-pin boundary conditions. Finally, different types of inhomogeneous materials should be analyzed for its buckling behavior, such as investigating the effect of anisotropy on the buckling mode, capacity, and behavior.

References

[1] W. G. Cooley,"Application of functionally graded materials in aircraft structures," M.Sc. thesis, Airforce Institute of Technology, Ohio, 2005.

[2] W. Pompe, H. Worch, M. Epple, W. Friess , M. Gelinsky, P. Greild, U. Hempel, D. Scharnweber and K. Schulte, "Functionally graded materials for biomedical applications," in *Materials Science and Engineering*,vol. 362, pp. 40-60, 2003.

[3] I. Elishakoff and O. Rollot, "New closed-form solutions for buckling of a variable stiffness column by Mathematica," in *Int J Sound and Vibration*, vol. 224, pp. 172-182, 1999.

[4] I. Elishakoff, "Inverse buckling problem for inhomogeneous columns",. Int J Solids and Structures, vol. 20, pp. 457-464, 2001.

[5] Q. S. Li, "Exact solutions for buckling of non-uniform columns under axial concentrated and distributed loading," in *J Mechanics and Solids*, vol. 20, pp. 485-500, 2001.

[6] Y. Huang and X. F. Li, "An analytical approach for exactly determining critical loads of buckling of nonuniform columns," in *J Structural Stability and Dynamics*, vol. 12, pp. 1-13, 2011.

[7] E. Atlus, A. Proskura and S. Givli, "A new functional perturbation method for linear non- homogeneous materials." in *Int J of Solids and Structures*, vol. 42, pp. 1577-1595, 2005.

[8] Y. Huang and Q. Luo, "A simple method to determine the critical buckling loads for axially inhomogeneous beams with elastic restraint," in *Computer and mathematics with applications,* vol. 61, pp. 2510-2517, 2011.

[9] T. Morimoto and Y. Tanigawa, "Linear buckling analysis of orthotropic inhomogeneous rectangular plates under uniform in-plane compression," in *Acta Mechanica*, vol. 187, pp. 219-229, 2006.

[10] C. J. Earls, "Observations on eigenvalue buckling analysis within a finite element context," in *Proceedings of the SSRC Annual Stability Conference*, New Orleans, LA, 2007.

[11] X. F. Li, L.Y. Xi and Y. Huang, "Stability analysis of composite columns and parameter optimization against buckling," in *Composites*, vol. 42, pp. 1337-1345, 2011.

[12] I. Elishakoff and I. Calio, "Closed-form solutions for axially graded beam-columns," in *Int J Sound and Vibrations,* vol. 280, pp. 1083-1094, 2005.

[13] I. Elishakoff and C. Bert, "Comparison of Rayleighs noninteger-power method with Rayleigh Ritz method," in *Computer Methods in Applied Mechanics and Engineering*, vol. 67, pp. 297-309, 1988.

[14] S. Pradhan and S. Chakraverty, "Free vibration of Euler and Timoshenko functionally graded beams by Rayleigh-ritz method," in *Composites*, vol. 51, pp. 175-184, 2013.

[15] B. Sankar, "An elasticity solution for functionally graded beams," in *Composite science and technology*, vol. 61, pp. 689-696, 2001.

[16] I. Elishakoff and Y. Miglis, "Some intriguing results pertaining to functionally graded columns," in *J Applied Mechanics*, vol. 80, pp. 1-6, 2013.

[17] Y. Huang and X. F. Li, "A new approach for free vibration of axially functionally graded beams with non-uniform cross-section," in *J Sound and Vibrations*, vol. 329, pp. 2291-2303, 2010.

[18] G. Swenson, "Analysis of nonuniform columns and beams by a simple dc network analyzer," in *J Aeronautical Sciences*, vol.19, pp. 273-275, 1952.

[19] S. Coskun and M. Atay, "Determination of critical buckling load for elastic columns of constant and variable cross-sections using variation iteration method," in *Computer and Mathematics with Applications*,vol. 58, pp. 2260-2266, 2009.

[20] O. Oyekoyaet, D. Mba and A. El-Zafarany, "Buckling and vibration analysis of functionally graded composite structures using the finite element method," in *Composite Structures*, vol. 89, pp. 134-142, 2009.

[21] Z. Zhong and T. Yu, "Analytical solution of cantilever functionally graded beam," in *Composites Science and Technology,* vol. 67, pp. 481-488, 2007.

[22] Y. Yilmaz, Z. Girigin and S. Evran, "Buckling analyses of axially functionally graded   nonuniform columns with elastic restraint using a localized differential quadrature method," in *Mathematical Problems in Engineering*, vol. 2013, pp. 1-12, 2013.

[23] G. Chandran and M. Rajendran, "Study on buckling of column made of functionally graded material," in *Proceedings of IRF Conference*, pp. 32-34, 2014.

[24] K. Singh and G. Li, "Buckling of functionally graded and elastically restrained non-uniform columns," in *Composites*, vol. 40, pp. 393-403, 2009.

[25] Y. Hunag and X. Li, "Buckling of functionally graded circular columns including shear deformation," in *Materials and Design*, vol. 31, pp. 3159-3166, 2010.

[26] H. Ding, D. Huang and W.Q. Chen, "Elasticity solutions for plane anisotropic functionally graded beams," in *Int J Solids and Structures*, vol. 44, pp. 176-196, 2007.

[27] B. Shariat and M. Eslami, "Buckling of thick functionally graded plates under mechanical and thermal loads," in *Composite Structures*, vol. 78, pp. 433-439, 2007.

[28] E. Bagherizadeh, Y. Kiani and M.R. Eslami, "Mechanical buckling of functionally graded material cylindrical shells surrounded by Pasternak elastic foundation," in *Composite Structures*, vol. 93, pp. 3063-3071, 2011.

[29] S. R. Li and R. Batra, "Relations between buckling loads of functionally graded Timoshenko and homogenous Euler-Bernouli beams," in *Composite Structures*, vol. 95, pp. 5-9, 2012.

[30] R. Kadoli, K. Akthar and N. Ganesan, "Static analysis of functionally graded beams using higher order shear deformation theory," in *Applied Mathematical Modelling*, vol. 32, pp. 2509-2525, 2008.

[31] A. Heydari, "Buckling of functionally graded beams with rectangular and annular sections subjected to axial compression," in *Advanced Design and Manufacturing Technology*, vol. 5, pp. 25-31, 2011.

[32] ABAQUS, *User Manual 6.3*, Providence, RI, Habbitt, Karlsson and Sorensen, Inc., 2004.

[33] M. Ostoja-Starzewski, "Random field models of heterogeneous materials," in *Solid Structures*, vol. 35, pp. 2429-2455, 1998.

[34] S. Schnabl S and I. Planinc, "The effect of transverse shear deformation on the buckling of twolayer composite columns with interlayer slip," in *Int J non-linear mechanics*, vol. 46, pp. 1-39, 2011.

[35] R. Cook, D. Malkus, M. Plesha and R. Witt, *Concepts and Applications of Finite Element Analysis*, John Wiley & Sons, 2007.

Appendix

Table A.1: Function parameters for bilinear, $sin^2(x)$, sin, cubic functions

Bilinear				$E(x) = [\sin(x)]^2$	
a (MPa)	b($\dfrac{MPa}{mm}$)	c (MPa)	d($\dfrac{MPa}{mm}$)	a (MPa)	b (MPa)
0	149	597000	-149	0	300000
10000	140	570000	-140	10000	280000
20000	130	540000	-130	20000	260000
30000	120	510000	-120	30000	240000
40000	110	480000	-110	40000	220000
50000	100	450000	-100	50000	200000
60000	90	420000	-90	60000	180000
70000	80	390000	-80	70000	160000
80000	70	360000	-70	80000	140000
90000	60	330000	-60	90000	120000
100000	50	300000	-50	100000	100000
Cubic				$E(x) = \sin(x)$	
a($\dfrac{MPa}{mm^3}$)	b($\dfrac{MPa}{mm^2}$)	c($\dfrac{MPa}{mm}$)	d (MPa)	a (MPa)	b (MPa)
0	-0.05625	225	0	0	353429.174
0	-0.0525	210	10000	10000	329867.229
0	-0.04875	195	20000	20000	306305.284
0	-0.045	180	30000	30000	282743.339
0	-0.04125	165	40000	40000	259181.394
0	-0.0375	150	50000	50000	235619.449
0	-0.03375	135	60000	60000	212057.504
0	-0.03	120	70000	70000	188495.559
0	-0.02625	105	80000	80000	164933.614
0	-0.0225	90	90000	90000	141371.669
0	-0.01875	75	100000	100000	117809.725

Table A.2: Function parameters for quadratic and power functions

Quadratic			Power		
$a\,(\frac{MPa}{mm^2})$	$b\,(\frac{MPa}{mm})$	$c\,(MPa)$	a	b	$c\,(MPa)$
-0.0525	210	10000	1.135	0.8174	0
-0.04875	195	20000	1.138	0.8131	10000
-0.045	180	30000	1.142	0.8084	20000
-0.04125	165	40000	1.146	0.8033	30000
-0.0375	150	50000	1.15	0.7978	40000
-0.0338	135	60000	1.155	0.7918	50000
-0.03	120	70000	1.161	0.7851	60000
-0.02625	105	80000	1.167	0.7777	70000
-0.0225	90	90000	1.173	0.7693	80000
-0.01875	75	100000	1.181	0.7595	90000
-0.015	60	110000	1.191	0.748	100000

Vita

Mohammed G. Aldadah was born 1990 in Fujairah, United Arab Emirates. He received his high school diploma from Fujairah Islamic Scientific School in Fujairah. In 2011, he graduated from the American University of Sharjah with a bachelor's degree in mechanical engineering with a GPA of 3.29. Then, Mohammed joined the Master of Science in Mechanical Engineering program in the American University of Sharjah. He received a full scholarship and worked as a graduate research and teaching assistant.